Genetic Screens for *Caenorhabditis elegans* Mutants Defective in Left/Right Asymmetric Neuronal Fate Specification

Sumeet Sarin,[1] M. Maggie O'Meara,[1] Eileen B. Flowers,[1] Celia Antonio,[1] Richard J. Poole, Dominic Didiano, Robert J. Johnston, Jr., Sarah Chang, Surinder Narula and Oliver Hobert[2]

Howard Hughes Medical Institute, Department of Biochemistry and Molecular Biophysics, Columbia University Medical Center, New York, New York 10032

ABSTRACT

We describe here the results of genetic screens for *Caenorhabditis elegans* mutants in which a single neuronal fate decision is inappropriately executed. In wild-type animals, the two morphologically bilaterally symmetric gustatory neurons ASE left (ASEL) and ASE right (ASER) undergo a left/right asymmetric diversification in cell fate, manifested by the differential expression of a class of putative chemoreceptors and neuropeptides. Using single cell-specific *gfp* reporters and screening through a total of almost 120,000 haploid genomes, we isolated 161 mutants that define at least six different classes of mutant phenotypes in which ASEL/R fate is disrupted. Each mutant phenotypic class encompasses one to nine different complementation groups. Besides many alleles of 10 previously described genes, we have identified at least 16 novel *"lsy"* genes (*"laterally symmetric"*). Among mutations in known genes, we retrieved four alleles of the miRNA *lsy-6* and a gain-of-function mutation in the 3′-UTR of a target of *lsy-6*, the *cog-1* homeobox gene. Using newly found temperature-sensitive alleles of *cog-1*, we determined that a bistable feedback loop controlling ASEL *vs.* ASER fate, of which *cog-1* is a component, is only transiently required to initiate but not to maintain ASEL and ASER fate. Taken together, our mutant screens identified a broad catalog of genes whose molecular characterization is expected to provide more insight into the complex genetic architecture of a left/right asymmetric neuronal cell fate decision.

APART from expressing a core set of features that distinguish neuronal from nonneuronal cell types, individual cell types in the nervous system express distinct batteries of genes that generate the structural and functional diversity of neuronal cell types. The diversification of cell fate in the developing nervous system presumably relies on the interplay of a host of regulatory factors. Screens for mutant animals defective in neuronal fate specification provide a powerful and unbiased approach to identify these regulatory factors. Such screens have been successfully conducted in various model systems, most prominently flies and worms, yielding valuable insights into the molecular mechanisms that control neuronal fate specification. We describe here genetic screens for neuronal fate mutants in the nematode *Caenorhabditis elegans* that focus on a cell fate decision executed by a single neuron class, the ASE gustatory neurons. This neuron class is composed of two morphologically bilaterally symmetric neurons, ASE

left (ASEL) and ASE right (ASER). ASEL and ASER are the main taste receptor neurons of *C. elegans* and sense multiple chemosensory cues in a left/right asymmetric manner (BARGMANN and HORVITZ 1991; PIERCE-SHIMOMURA *et al.* 2001) (our unpublished data). Left/right asymmetric chemosensory functions correlate with the left/right asymmetric expression of a class of putative chemoreceptors encoded by the *gcy* (*guanylyl cyclase*) gene family (YU *et al.* 1997; PIERCE-SHIMOMURA *et al.* 2001; ORTIZ *et al.* 2006) (Figure 1). These left/right asymmetric features of ASEL and ASER provide a model to understand how functional laterality is superimposed on a morphologically symmetric structure, a hallmark of many nervous systems across phylogeny (HOBERT *et al.* 2002; SUN and WALSH 2006).

We have previously reported the identification of mutants that affect the development of the left/right asymmetry of the ASE neurons (CHANG *et al.* 2003; JOHNSTON and HOBERT 2003, 2005; JOHNSTON *et al.* 2006). These mutants, which we termed *lsy* mutants (for *laterally symmetric*) to indicate their role in controlling the fate of two left/right asymmetric neurons, fell into four distinct classes (Figure 1A). In class I mutants, both ASE neurons adopt the fate of the ASEL neuron, with a concomitant loss of ASER cell fate ("2 ASEL" mutants). In
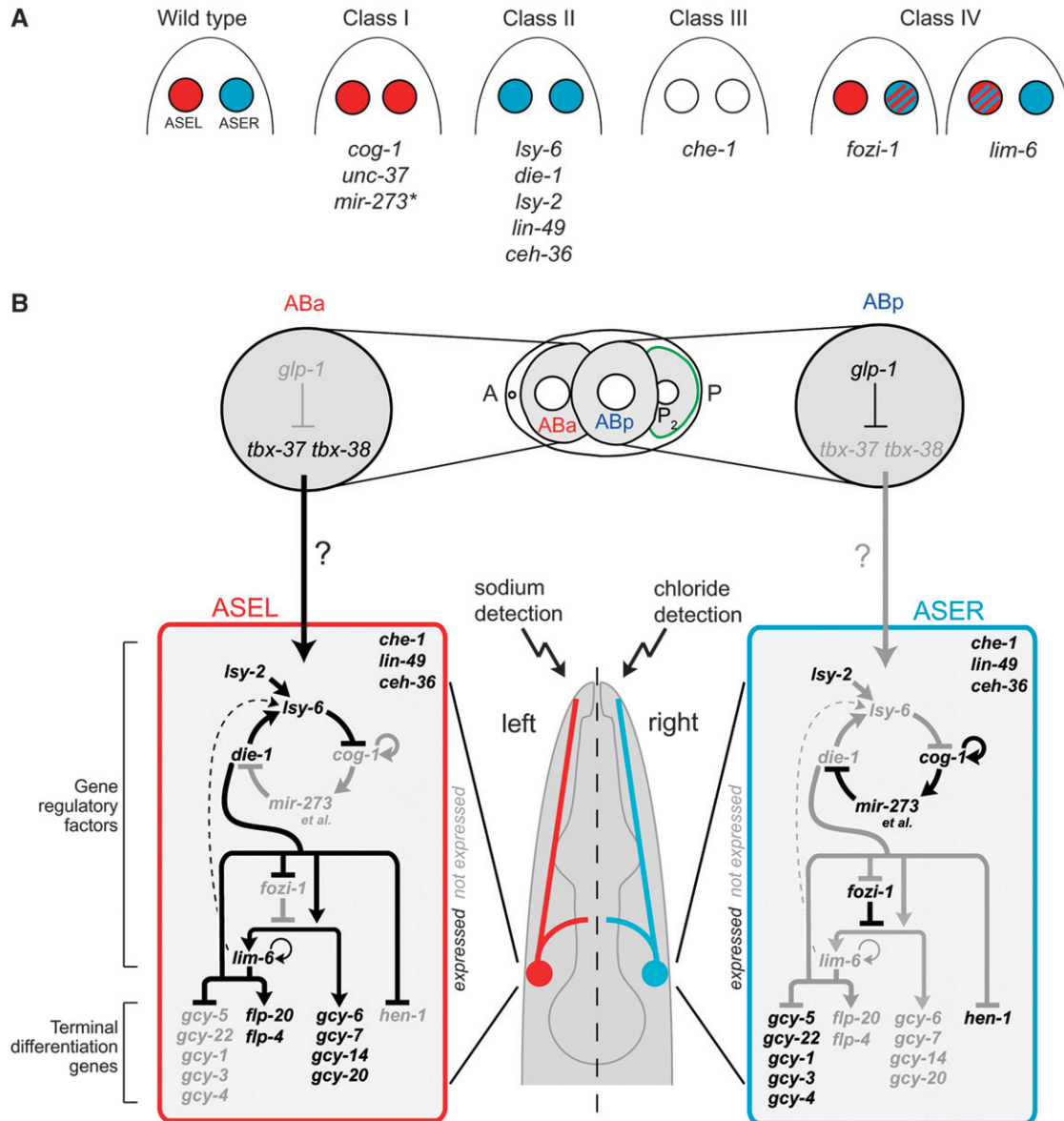
FIGURE 1.—Summary of the ASEL/R differentiation program. (A) Schematic of mutant classes previously identified in screens for ASEL/R developmental defects. Red indicates ASEL fate, monitored with several distinct *gfp* markers, and blue indicates ASER fate. The asterisk indicates that *mir-273* is inferred to be an inducer of ASER fate based on gain-of-function, rather than loss-of-function phenotypes (CHANG *et al.* 2004). See text for more explanations of the phenotypes. (B) ASEL/R laterality is controlled by a bistable regulatory feedback loop (HOBERT 2006). The bias in the activity of the regulatory loop can be traced back to the four-cell stage in which the two precursors of ASEL (ABa) and ASER (ABp) are instructed by a Notch signal, emanating from the P2 cell, to adopt distinct fates (POOLE and HOBERT 2006). *lsy-2, ceh-36*, and *lin-49* are required for execution of the ASEL fate, but are not instructive since they are expressed in both ASEL and ASER (CHANG *et al.* 2003). Why these genes are not active in ASER and how they control the expression of individual genes in this network is not currently known. UNC-37, a transcriptional corepressor, likely physically interacts with COG-1 and is not shown here. *che-1* is also expressed in ASEL and ASER and appears to control the expression of every gene in this regulatory network (CHANG *et al.* 2003; ETCHBERGER *et al.* 2007).

class II mutants, the opposite phenotype is observed, with both neurons expressing ASER fate and losing ASEL fate ("2 ASER" mutants). In class III mutants, both ASEL and ASER fates are lost and in class IV mutants, either the ASEL or the ASER fate is mixed, expressing both ASEL and ASER features (Figure 1A). The molecular characterization of these mutants revealed a complex gene regulatory network composed of several

transcription factors and miRNAs that control ASEL/R fate specification (Figure 1B) (HOBERT 2006). These regulatory factors interact with one another in specific network configurations, including feedback and feed-forward loops, to control ASEL/R fate specification (HOBERT 2006). Given that both cells have the ability to adopt either the ASER or the ASEL fate, the system essentially classifies as a bistable system (JOHNSTON *et al.*

2005). Conceptually similar bistable systems that also utilize double-negative feedback loops composed of gene regulatory factors include the decision of phage lambda to adopt either the lytic or the lysogenic state (PTASHNE 1992).

ASEL and ASER fates are adopted after the two neurons have passed through a transient hybrid precursor state. During the hybrid precursor state, both neurons coexpress genes that during ensuing development become restricted to either ASEL or ASER (JOHNSTON *et al.* 2005). However, the decision regarding which of the two ASE neurons adopts the stable ASER or ASEL fate is not controlled at the stage when the ASE neurons progress from the hybrid precursor state to their terminal state. It is rather determined very early in embryogenesis by a signal sent along the anterior/posterior axis through the *glp-1*/Notch signaling system (Figure 1B) (POOLE and HOBERT 2006). This signal represses expression of two T-box genes at the four-blastomere stage (GOOD *et al.* 2004), thereby instructing a descendant of the ABa blastomere to eventually adopt the ASEL fate and a descendant of the ABp blastomere to adopt the ASER fate (Figure 1B) (POOLE and HOBERT 2006). Since the Notch signal and the eventual adoption of the ASEL and the ASER fate are separated by nine cell divisions, one central unanswered question is how this information is transmitted throughout development (indicated by a "?" in Figure 1B).

Genetic screens for mutants that affect ASEL/R fate specification may not only provide the link between early embryonic signaling and terminal neuron specification but also reveal additional components of the bistable loop shown in Figure 1B. Since the bistable feedback loop involves several miRNAs, a class of regulatory molecules whose mechanism of action is poorly understood (NILSEN 2007), another expected outcome of genetic screens for ASE specification mutants is the discovery of molecules that may act together with miRNAs to control the expression of their target genes.

In this article, we provide a first step toward these goals by reporting the results of significantly expanded genetic screening efforts aimed at uncovering the complete genetic regulatory architecture required for ASEL/R fate specification. Previously published mutants (CHANG *et al.* 2003; JOHNSTON and HOBERT 2003, 2005; JOHNSTON *et al.* 2006) were derived from relatively small-scale screens totaling ∼15,000 haploid genomes (Table 1). We describe here mutants from those previous screens that were not yet reported and report the results of an almost 10-fold expansion of these screening efforts, resulting in the screening of ∼120,000 haploid genomes (Table 1). We describe informative alleles of previously known genes, such as temperature-sensitive alleles that allowed us to determine the timing of action of the bistable feedback loop described above. We describe new genes that fall into previously described phenotypic categories as well as genes that define novel phenotypic categories.

TABLE 1

Overview of screens for *lsy* mutants

Reporter	Transgene	Haploid genomes screened	No. of alleles
ASEL reporter *lim-6^{prom}::gfp*	*otIs6*	3,200	11[a]
	otIs114	84,600	116[b]
ASEL reporter *gcy-7^{prom}::gfp*	*otIs3*	12,200	19[c]
ASER reporter *gcy-5^{prom}::gfp*	*ntIs1*	19,440	15[b]

Total: 119,440 Total: 161
Allele frequency: 1/740 haploid genomes

[a] Five of these 11 alleles were molecularly analyzed in CHANG *et al.* (2003, 2004) [*cog-1(ot28)*, *cog-1(ot38)*, *unc-37(ot59)*, *die-1(ot26)*, and *che-1(ot27)*]. The remaining 6 alleles (*ot25*, *ot29*, *ot30*, *ot31*, *ot35*, and *ot37*) are described in this article.

[b] First described in this article.

[c] Sixteen of these 19 alleles were molecularly analyzed in CHANG *et al.* (2003) (*cog-1*, *lin-49*, *ceh-36*, and *che-1*), JOHNSTON and HOBERT (2003) (*lsy-6*), JOHNSTON and HOBERT (2005) (*lsy-2*), and JOHNSTON *et al.* (2005) (*fozi-1*). The remaining 3 alleles (*ot68*, *ot76*, *ot80*) are described in this article.

Our mutant collection illustrates the genetic complexity of neuronal cell fate decisions.

MATERIALS AND METHODS

Strains and reporter transgenes: N2 Bristol wild-type (BRENNER 1974) and CB4856 Hawaiian wild-type isolates (HODGKIN and DONIACH 1997) were used. Transgenes that label ASEL and ASER fates include ASEL markers *otIs3V = Is[gcy-7^{prom}::gfp; lin-15 (+)]*, *otIs131 = Is[gcy-7^{prom}::dsRed2; rol-6(d)]*, *otIs6*, and *otIs114I = Is[lim-6^{prom}::gfp; rol-6(d)]*; ASER markers *ntIs1V = Is[gcy-5^{prom}::gfp; lin-15 (+)]* and *otEx2333 = Ex[gcy-5^{prom}::cherry, rol-6(d)]*; and ASEL/R marker *otIs151V = Is[ceh-36^{prom}::rfp; rol-6(d)]*. Reporter transgenes that assay the 3′-UTR regulation in ASEL *vs.* ASER are *otEx2646 = Ex[ceh-36^{prom}::gfp::unc-54^{3′-UTR}]* and *otIs185 = Is[ceh-36^{prom}::gfp::cog-1^{3′-UTR}]*.

Screening for *lsy* mutants: In all screens, animals were mutagenized with EMS according to standard protocols (BRENNER 1974), one to two F$_1$ progeny of mutated P0 animals were singled on individual plates, and their ensuing progeny (F$_2$ and F$_3$ generation) were screened under a stereomicroscope equipped with a fluorescent light source. Animals with mutant phenotypes were picked, and their Lsy phenotype was confirmed in ensuing generations and subsequently backcrossed [alleles of previously characterized genes were generally backcrossed zero to two times, and new *lsy* genes and the *cog-1(ot221ts)* allele were backcrossed two to five times] and then mapped. Temperature sensitivity was tested by maintaining mutant animals for several generations at 15° and 25° before scoring.

As indicated in Table 1, four independent screens were conducted using three different L/R asymmetric fate reporters, expressed from four different chromosomally integrated transgenic arrays, *lim-6^{prom}::gfp* (*otIs114* and *otIs6*), *gcy-7^{prom}::gfp* (*otIs3*) (all ASEL markers), and *gcy-5^{prom}::gfp* (*ntIs1*; ASER marker). Each reporter has its own individual advantages and disadvantages. While all markers are visible under a stereomicroscope equipped with a fluorescent light source, the ASEL

reporters *lim-6^{prom}::gfp* and *gcy-7^{prom}::gfp* produce substantially more *gfp* fluorescence than the ASER reporter *gcy-5^{prom}::gfp*. To facilitate the screening through a large number of genomes, we therefore conducted most of our screens (100,000/119,440 haploid genomes) with ASEL markers. Among those markers, we preferred *lim-6^{prom}::gfp* over *gcy-7^{prom}::gfp* since the strong expression of *lim-6^{prom}::gfp* in the excretory gland cells provides a convenient internal control to exclude that loss of *lim-6^{prom}::gfp* expression in ASEL is not simply caused by global array loss. *lim-6^{prom}::gfp* integrants also appear to be more healthy than several independently derived *gcy-7^{prom}::gfp* integrants. One shortcoming of the usage of the ASEL markers *gcy-7* or *lim-6* for screening is that in embryos, these markers are bilaterally expressed in ASEL and ASER and become restricted to ASEL only postembryonically (JOHNSTON *et al.* 2005). Mutant animals that arrest at embryonic stages can therefore only be assessed for the absence of *gfp* expression, but not for aberrant expression of ASEL fate in ASER, observed in class I (2 ASEL) mutants in larval and adult stages. This problem cannot be easily overcome through the use of *gcy-5^{prom}::gfp*, which is restricted to ASER even in embryos, since 2 ASEL mutants would produce mutants that fail to express *gcy-5^{prom}::gfp*. In practice, such non-*gcy-5^{prom}::gfp*-expressing, arrested embryos are difficult to identify in a large population of mutagenized animals. Non-*gcy-5^{prom}::gfp*-expressing, arrested embryos may have also simply died before the ASE neurons are born. Since we attempted to be as unbiased as possible in our phenotypic categories, we nevertheless also screened a substantial number of genomes with *gcy-5^{prom}::gfp* (Table 1). The use of several independent *gfp* arrays also controls for possible genetic background effects in the transgenic strains.

The screens with the *otIs6*, *otIs3*, and *ntIs1* transgenes (34,840 haploid genomes screened) were conducted at 20° (*i.e.*, animals were constantly maintained at this temperature) while the screen with the *otIs114* transgene (84,600 haploid genomes screened) was conducted at 25° to allow for the isolation of temperature-sensitive alleles. For the screen with *ntIs1*, a *gcy-7^{prom}::rfp* transgene (*otIs131*) was contained in the background. *Rfp* expression from this array is too low to allow for primary screening under a stereo microscope, but this transgene allows us to quickly distinguish under a compound microscope whether aberrant *gcy-5^{prom}::gfp* expression was paralleled by aberrant ASEL marker expression. As the *otIs131* array contained a dominant roller mutation, this array also facilitated the assessment of left/right asymmetric *gcy-5^{prom}::gfp* expression since animals can be observed from multiple distinct perspectives.

Mapping and allele identification: We first tested mutants for linkage to the X chromosome by crossing them with wild-type males and examining a potential mutant phenotype in hemizygous, male F_1 cross-progeny. If a phenotype was observed in the F_1 male progeny, it was tested whether this is due to dominance rather than to X-linkage. If a mutant was indeed X-linked, it was, depending on the mutant phenotypic class, either complementation tested or sequenced to determine whether it was allelic to known X-linked genes with a Lsy phenotype (*ceh-36*, *lsy-2*, *lim-6*). If the mutant was not X-linked, a mapping strategy was employed that was contingent on the known set of previously identified, non-X-linked genes involved in ASE fate specification (class I, *cog-1*, *unc-37*; class II, *lin-49*, *die-1*, *lsy-6*; class III, *che-1*; class IV, *fozi-1*) (CHANG *et al.* 2003, 2004; JOHNSTON and HOBERT 2003, 2005; JOHNSTON *et al.* 2006). Each mutant that failed to express one of the ASEL or ASER fate markers could, depending on the *gfp* marker used, constitute either a class III ("no ASE differentiation") or a class I or II phenotype (loss of either ASEL or ASER fate, with inappropriate execution of the opposite cell fate). To avoid remapping already known genes, we did not cross further *gfp*

markers into the individual mutants to precisely define that phenotype, but rather immediately conducted complementation tests. All mutants with a lack of expression of either a left- or a right-specific *gfp* fate marker were first complemented with the sole gene that defines the class III mutant class, *che-1*. A failure to complement was followed by sequencing of the *che-1* locus. If the mutant complemented *che-1*, further complementation tests were contingent on the transgenic array and the mutant phenotype. Mutants that constituted a potential class II phenotype (2 ASER phenotype; *i.e.*, bilateral expression of the ASER marker *gcy-5* or loss of expression of the ASEL marker *lim-6* or *gcy-7*) were complemented against known, non-X-linked class II genes (*die-1*, *lsy-6*, *lin-49*); failure to complement was followed by sequencing of the respective loci. Mutants that constituted a potential class I phenotype (2 ASEL phenotype; *i.e.*, bilateral expression of ASEL marker *gcy-7* or *lim-6* or lack of expression of ASER marker *gcy-5*) were initially not complementation tested against known class I genes since we had found that the first two described class I mutants, *cog-1* and *unc-37*, displayed nonallelic noncomplementation (CHANG *et al.* 2003; in the course of characterizing new class I mutants, we subsequently found that nonallelic noncomplementation is not a general feature of all class I genes; supplemental Table 2 at http://www.genetics.org/supplemental/). New class I mutants were therefore rather linked to individual chromosomes using single-nucleotide polymorphisms (SNPs) in the CB4856 Hawaiian wild-type isolate (WICKS *et al.* 2001; SWAN *et al.* 2002; DAVIS *et al.* 2005). If located on the same chromosome as *cog-1* (LGII), *unc-37* (LGI), or *fozi-1* (LGIII; this is a different mutant class, but like class I mutants, it also displays ectopic expression of ASEL markers in ASER), the respective loci were sequenced, leading to the identification of 28 alleles of the previously known *cog-1*, *unc-37*, and *fozi-1* genes.

Mutants that were not allelic to previously known genes were further mapped using SNP markers (supplemental Table 2 at http://www.genetics.org/supplemental/). Mutants locating in similar intervals were complementation-tested against each other (supplemental Table 2). With the exception of X-linked and dominant genes, these complementation tests, as well as complementation tests mentioned above, were usually done by crossing two mutants and determining whether F_1 male cross-progeny displayed the mutant phenotype.

Reporter gene constructs: The functional consequence of the *lsy-6(ot150)* promoter mutation was tested by introducing this mutation into a reporter construct that monitors expression in ASEL. The wild-type reporter construct was generated by subcloning a 930-bp PCR product, extending from −930 to −1 bp relative to the *lsy-6* hairpin into the pPD95.75 expression vector, using an *Xba*I site and a *Hin*dIII site introduced at either end of the PCR product. This construct, termed *lsy-6^{promC}::gfp*, contains the same sequences as the previously described *lsy-6* promoter construct *lsy-6^{prom}::gfp* (incorrectly annotated in JOHNSTON and HOBERT 2003 as containing 2 kb of promoter sequence). In contrast to the previously described *lsy-6^{prom}::gfp*, which was generated by PCR fusion and injected with a *rol-6(d)* injection marker, *lsy-6^{promC}::gfp* was subcloned and was injected at 50 ng/μl with 45 ng/μl *elt-2::gfp* injection marker. We note that *lsy-6^{prom}::gfp* transgenes [both extrachromosomal arrays and the integrated derivative *otIs160* (JOHNSTON *et al.* 2005)] are expressed with high penetrance in ASEL and also in a few other head and tail neurons (JOHNSTON and HOBERT 2003), while four different *lsy-6^{promC}::gfp* extrachromosomal arrays (*otEx3071*, *otEx3072*, *otEx3079*, and *otEx3080*) produce lowly penetrant (12–33%) expression in ASEL, generally lower *gfp* levels in ASEL and no readily detectable *gfp* expression in other neurons. These differences in *gfp* expression may be due to differences in copy

numbers of the DNA on the arrays (linear DNA is more efficiently incorporated on DNA than circular DNA) or to the usage of different injection markers.

The *lsy-6^{promC}::gfp* construct was mutated using the Stratagene (La Jolla, CA) QuickChange II XL site-directed mutagenesis kit to introduce the *ot150* allele into the reporter construct. Like the wild-type construct, this construct was also injected at 50 ng/μl with 45 ng/ul *elt-2::gfp* injection marker.

Primer sequences (5′–3′) for these constructs are as follows:

lsy-6prom5′ *Hin*dIII: ttaagcttCTTCTGACGAACCAAAGCC
lsy-6prom3′ *Xba*I: GCTTATTTTTCAGAAATTAGTAGGtctagaaa
lsy-6promot150mut5′: ggtgcctgatatttacggctttcgcccattaccg
lsy-6promot150mut3′: cggtaatgggcgaaagccgtaaaatatcaggcacc.

For the 3′-UTR sensor construct, two previously described control sensor constructs (*cog-1* 3′-UTR and *unc-54* 3′-UTR) were rescored (DIDIANO and HOBERT 2006). A *cog-1* 3′-UTR sensor construct replicating the *ot123* deletion was generated by PCR amplification (see primer sequences below) of the wild-type *cog-1* 3′-UTR; the amplicon was digested with *Eag*I and *Eco*RI and was used to replace the *unc-54* 3′-UTR in the previously described *ceh-36^{prom}* sensor construct (DIDIANO and HOBERT 2006). The sensor construct was injected at 5 ng/μl with *rol-6(d)* at 100 ng/μl as the injection marker.

Primer sequences (5′–3′) for these constructs are as follows:

DD#97: tttgaattcctttaagcgttctacctct
DD#415: ttttcggccggtttggtTTTTGTATAAGTGACGATGATTTGG.

All sensor construct-expressing strains were maintained at 20° prior to scoring. All lines were scored under a Zeiss Axioplan 2 microscope. To minimize the inclusion of mosaic animals only those animals were scored in which *gfp* expression in the AWCL and AWCR neurons was observed. The fluorescence intensity of the 3′-UTR sensor constructs was compared between ASEL and ASER in each individual animal and scored as ASEL > ASER, ASEL = ASER, or ASER > ASEL (see DIDIANO and HOBERT 2006 for a more detailed explanation of scoring criteria).

Microscopy, laser ablation, and phenotypic observations: Laser ablations were done as previously described (POOLE and HOBERT 2006). Embryos were dissected from gravid hermaphrodites, mounted at the one- to four-cell stage in a drop of water on a 5% agar or agarose pad, and sealed between a coverslip and slide using melted Vaseline. A Photonics dye laser attached to the microscope was used to ablate embryonic blastomeres. Larger early blastomeres were irradiated for 3–5 min with the laser beam, while smaller later blastomeres were irradiated for 1–2 min in and around the nucleus. Increased cytoplasmic movements were often observed and in many cases the nucleus was observed to break down. Irradiated blastomeres usually did not divide although on some occasions late aberrant divisions were observed. Laser ablations were performed at 25°. A copper ring attached to the microscope objective through which temperature-controlled water was passed maintained the constant temperature of the slide. Following ablation the slides were left overnight for ~12–15 hr at 25° and then scored for the number of cells exhibiting transgene expression at late threefold/L1 stages.

RESULTS AND DISCUSSION

Overview of the screen

We used three different L/R asymmetrically expressed *gfp* reporter genes to monitor ASEL or ASER fate. *lim-6^{prom}::gfp* is expressed in ASEL and in the excretory gland

cells, *gcy-7^{prom}::gfp* is expressed in ASEL and weakly in the excretory cell of adult animals, and *gcy-5^{prom}::gfp* is expressed exclusively in ASER. We conducted separate F_1 semiclonal screens for mutants in which the expression of the respective *gfp* marker is different from expression in wild-type animals (see MATERIALS AND METHODS for a detailed description of the screen and for an explanation on why different markers were used). A total of 119,440 haploid genomes were screened (100,000 with ASEL markers and 19,440 with an ASER marker) and 161 mutants with *gfp* expression defects were retrieved (Table 1). Mutant phenotypes are 2–100% penetrant. We focused our analysis on 123 mutants. The other mutants were not pursued since they display defects that are <10% penetrant (34 mutants), have multiple loci mutated (2 mutants), or have the *gfp*-expressing array affected (2 mutants) (supplemental Table 1, A–C, at http://www.genetics. org/supplemental/). Most of the isolated mutant strains were viable and recessive (Table 3). By complementation testing, mapping, and allele sequencing (see MATERIALS AND METHODS), these 123 alleles were found to define 30 complementation groups (Tables 2 and 3; supplemental Table 2 at http://www.genetics.org/supplemental/). The mutation rate of 1 mutant allele per 740 haploid genomes is within the range of the average mutation rate observed in other mutant screens (ANDERSON 1995).

We observed six mutant classes that show aberrant expression of ASEL/R fate markers (classes I–VI), two of which had not been previously described (class V and class VI) (Figure 2). All mutant classes can be summarized as follows. As mentioned in the Introduction (Figure 1A), in class I mutants, ectopic expression of the ASEL fate is observed in ASER with concomitant loss of the ASER fate markers (*i.e.*, *lim-6^{prom}::gfp* or *gcy-7^{prom}::gfp* is expressed in two cells rather than one cell and *gcy-5^{prom}::gfp* expression is lost); in class II mutants, the opposite phenotype is observed; in class III mutants ASEL and ASER cell fate is not executed (*lim-6^{prom}::gfp*, *gcy-7^{prom}::gfp*, and *gcy-5* not expressed); and in class IV mutants ("mixed fate"), ASEL fate is ectopically expressed in ASER, but the ASER fate marker continues to be expressed (or, vice versa, ASER fate is ectopically expressed in ASEL with ASEL fate markers being unaffected) (Figure 1A). In two mutant classes not previously described, we observe a "heterogeneous phenotype" with a combination of loss and gain of *gfp* expression of individual markers in ASEL or ASER within a mutant population (class V mutants) and an ectopic *gfp* expression phenotype in which cells other than the ASE neurons express the cell fate marker (class VI mutants). In the following sections, we describe these mutants and phenotypic classes in more detail.

Class I mutants (2 ASEL neurons)

Alleles of known class I genes: We have isolated a total of 19 alleles of the previously known class I gene

TABLE 2

Summary of mutant classes and genes

Mutant class	ASE phenotype	No. genes	Gene names	Molecular identity	No. alleles
Class I	"2 ASEL"	6	*cog-1*	Homeobox	19
			unc-37	Corepressor	2
			lsy-5	Unknown	2
			lsy-22	Unknown	2
			lsy-16	Unknown	1
			lsy-17	Unknown	1
Class II	"2 ASER"	9	*die-1*	Zn-finger TF	9
			lsy-2	Zn-finger TF	5
			lsy-12	Unknown	5
			lsy-6	miRNA	4
			lin-49	Chromatin regulator	3
			lsy-14	Unknown	2
			lsy-15	Unknown	1
			lsy-19	Unknown	1
			ceh-36	Homeobox	1
Class III	No ASEL/R fate specification	1	*che-1*	Zn-finger TF	22
Class IV	Mixed fate in ASEL or ASER	5	*fozi-1*	Zn-finger TF	12
			lsy-18	Unknown	2
			lsy-20	Unknown	1
			lsy-26	Unknown	1
			lim-6	Homeobox	0[a]
Class V	Heterogeneous phenotype	2	*lsy-9*	Unknown	4
			lsy-21	Unknown	1
Class VI	Ectopic expression of ASER and/or ASEL fate marker in cell other than ASE neuron class	7	*ced-3*	CARD domain	12
			ced-4	CARD domain	5
			tax-2	Ion channel	1
			tax-4	Ion channel	1
			lsy-23	Unknown	1
			lsy-24	Unknown	1
			lsy-25	Unknown	1
Sum of mutants		30	16 novel		123

New genes are underlined. Mutants with <10% penetrance are not shown (see supplemental Table 1 at http://www.genetics.org/supplemental/).

[a] This gene is listed here since its knockout produces a class IV phenotype; we have not retrieved any alleles of this gene in our screening efforts.

cog-1, a homeobox gene (PALMER *et al.* 2002; CHANG *et al.* 2003), and 2 alleles of *unc-37*, the previously known *C. elegans* ortholog of the Groucho corepressor family (Table 3; Figure 3) (PFLUGRAD *et al.* 1997; CHANG *et al.* 2003). Each allele displays a characteristic 2 ASEL phenotype, manifested by the gain of ASEL markers in ASER and the concomitant loss of ASER markers in ASER (Figures 1A and 2A). Representative class I mutant animals display the phenotypic defects expected by the loss of ASER fate; *i.e.*, these mutants have defects in their ability to sense ASER-specific chemosensory cues (data not shown). This observation complements previous observations made with class II mutants (defective in ASEL-sensed cues; CHANG *et al.* 2004), class III mutants (defective in sensing both ASEL and ASER cues; UCHIDA *et al.* 2003), and class IV mutants (discrimination defects of ASEL and ASER cues; PIERCE-SHIMOMURA *et al.* 2001).

cog-1: Most *cog-1* alleles lie within the homeobox (Figure 3). We were unable to identify mutations in the coding region or UTRs of *cog-1* in two mutants, *ot119* and *ot201*, which we conclude are *cog-1* alleles because they (a) are tightly linked to the *cog-1* locus, (b) fail to complement a canonical *cog-1* mutation (supplemental Table 2 at http://www.genetics.org/supplemental/), and (c) are rescued by a fosmid, WRM067cF11, that contains the *cog-1* locus [two of seven lines rescue the 62%-penetrant 2 ASEL phenotype of *ot119* each to 15% ($n = 55$) and 7% ($n = 52$), respectively; two of eight lines rescue the 80%-penetrant 2 ASEL phenotype of *ot201* to 9% ($n = 51$) and 30% ($n = 65$), respectively]. These mutations may reside in regulatory elements that control *cog-1* expression.

By conducting most of the genetic screens at 25° (84,600 of the total of 119,440 haploid genomes

TABLE 3

List of *lsy* genes

Locus	Allele	Class	ASEL marker defect (%)	ASER marker defect (%)	Obvious pleiotropies	Map position	Notes	Nucleotide change	Sequence
						Linkage group I			
lsy-5	ot37[a]	Class I	62	74	Emb, Lvl, Ste, Unc, Pvl	−8.23– −5.78	Temperature sensitive	Uncloned	
	ot240		53		Unc, Pvl	−8.23– −5.78	Temperature sensitive	Uncloned	
lsy-17	ot190	Class I	22	26	Slow growth	Near −8	Temperature sensitive	Uncloned	
lsy-18	ot192[b]	Class IV	100	0	None obvious	Near −8	ASEL > ASER	Uncloned	
	ot247		50		None obvious		Temperature sensitive	Uncloned	
lsy-14	ot101	Class II	70	60	None obvious	1.24–1.29	ASEL defects most penetrant in adult	Uncloned	
	ot146		100		None obvious			Uncloned	
lsy-22	ot114	Class I	75	≥75[c]	Mel	9–13	Let but not Lsy is maternally rescued	Uncloned	
	ot244		100		Lvl, Ste, Unc			Uncloned	
lsy-26	ot104	Class IV	0	90	None obvious	−5–5		Uncloned	
che-1	ot27	Class III	100	100	None obvious	1.20	Temperature sensitive		CHANG *et al.* (2003)
	ot63		100		None obvious				CHANG *et al.* (2003)
	ot66		100		None obvious				CHANG *et al.* (2003)
	ot70		100		None obvious				CHANG *et al.* (2003)
	ot73		100		None obvious				CHANG *et al.* (2003)
	ot75		100		None obvious				CHANG *et al.* (2003)
	ot94[d]			87	None obvious			C > T	CAT AAA **TCT** TAT GTT
	ot95[d]			100	None obvious			C > T	CAT AAA **TCT** TAT GTT
	ot103			81	None obvious			G > A	taatttcaaTCA GAT
	ot124		100		None obvious			C > T	CAA AGT **TTT** TCT CTT
	ot135		100		None obvious			C > T	CCA TTT **TTT** CAA AGT
	ot144		100		None obvious			G > A	GGA GGA TGA CGA CAG
	ot145		100		None obvious			G > A	GGA GGA TGA CGA CAG
	ot151		100		None obvious			C > T	CAG GGA TAA AAT GGA
	ot152		100		None obvious			1-bp deletion	GAT TGG -AT TTC ACG
	ot153		100		None obvious			C > T	CCA TTT **TTT** CAA AGT
	ot167		100		None obvious			G > A	ATA CAG **atgagaagttt**
	ot173		100		None obvious			C > T	CAT AGG **TAC** ATG AAA
	ot178		100		None obvious			G > A	cttttcaa **GAGAAA**
	ot207		100		None obvious			C > T	CAT AAA **TCT** TAT GTT
	ot223		100		None obvious			C > T	TCT TCT **TTT** GTT ACT
	ot230		100		None obvious			G > A	TCA TTG ataagaa
	ot232		100		None obvious			C > T	AAT CCG **TAG** gtaattt
unc-37	ot59[e]	Class I	48	53	Unc, Mel	1.31			CHANG *et al.* (2003)
	ot243[e]		25		Unc, Mel			C > T	GCA CAA **TGA** AAG GAA
						Linkage group II			
die-1	ot26	Class II	100	100	None obvious	1.85			CHANG *et al.* (2004)
	ot100		100	100	None obvious				CHANG *et al.* (2004)
	ot108		69		Dpy			No mutation in coding region[f]	
	ot143		100		None obvious			G > A	GGA CCA **CAT** CAG CTG
	ot175		100		None obvious			G > A	GGA CCA **CAT** CAG CTG
	ot183		100		None obvious			C > T	GGA CCA **TGT** CAG CTG
	ot195		100		None obvious			G > A	GGA CCA **CAT** CAG CTG
	ot198		100		None obvious			C > T	CAA CTG CTT GTC CGA
	ot231		100		Dpy; poor male mating			C > T	GCT CTG **TAG** CTG ACA
lsy-24	ot120	Class VI	79[g]		Bags	Near 2		Uncloned	

(*continued*)

TABLE 3

(Continued)

Locus	Allele	Class	ASEL marker defect (%)	ASER marker defect (%)	Obvious pleiotropies	Map position	Notes	Nucleotide change	Sequence
lsy-15	*ot86*	Class II	70	66	Egl	−6.20− −1.79	Lsy is maternally rescued (Egl is not)	Uncloned	
lsy-21	*ot147*	Class V	12	0	Dpy	left of −14	Of ASE defective animals, 40% show apparent loss of ASE fate while 60% show ASEL loss	Uncloned	
cog-1	*ot28*	Class II	62	56		23.70			CHANG *et al.* (2003)
	ot38		100						CHANG *et al.* (2003)
	ot62		74				Semidominant		CHANG *et al.* (2003)
	ot91			25	Ste			C > T	GCA GAT TGT GCA CAG
	ot102		100					C > T	CAG TCC TAG TTA AAC
	ot107		50		Partially penetrant Ste, bags			G > A	ACA AAA TGA CGC AAG
	ot111		12		Ste			C > T	AAG AAG TAA AGC AGA
	ot116		62		None obvious			C > T	CAG TCC TAG TTA AAC
	ot119				None obvious			No mutation in coding region	aaaaccaaac/ggtctagaaa
	ot123(d)		100	100			Semidominant	3′-UTR deletion	CAG CTC GTC CAG GAG
	ot126		30		None obvious		Temperature sensitive	C > T	CAG CTC GTC CAG GAG
	ot155		40		Slightly Dpy		Temperature sensitive	C > T	GTT AAG ataggcatt
	ot193		100		Bags, Pvl			G > A	
	ot200		10		None obvious		Temperature sensitive	C > T	CAG CTC GTC CAG GAG
	ot201		80		None obvious			No mutation in coding region	
	ot218		100		Vul		Three mutations	A > T	GAG AGT CTA GTT AGG
	ot220		55		None obvious		Temperature sensitive	C > T	CAG CTC GTC CAG GAG
	ot221		55		None obvious		Temperature sensitive	C > T	CAG CTC GTC CAG GAG
	ot242		100		Bags, Pvl			G > A	aaattccaaTAAGCCG
fozi-1	*ot61*	Class IV	100	0	None obvious	Linkage group III 0.39			JOHNSTON *et al.* (2006)
	ot109		100		None obvious			C > T	CCA TGC TAT ATT CGA
	ot130		100		None obvious			C > T	CAG CAG TAG ATC ATA
	ot131		100		None obvious			C > T	CAA CAG TAG CAG CAA
	ot132		100		None obvious			C > T	CCA CTG TAG TCA ATT
	ot133		100		None obvious			C > T	CAA CTG TAG CAG CAA
	ot134		100		None obvious			C > T	AAT CAA TAG AAA CAA
	ot159		100		None obvious			G > A	gtttcaaATTCAA
	ot163		100		None obvious			C > T	CAA CAG TAG CAG CAA
	ot191		100		None obvious		More penetrant in adults	C > T	GTC ATG TAA CTT CTA
	ot234		65		None obvious			C > T	AAA CTG CTA TGC CAT
	ot236		100		None obvious			C > T	AAA CTG CTA TGC CAT
lin-49	*ot69*	Class II	53	100	Larval lethal	Linkage group IV 3.92			CHANG *et al.* (2003)
	ot74		57	81					CHANG *et al.* (2003)
	ot78		59	61					CHANG *et al.* (2003)
lsy-25	*ot97*	Class VI	28	56[a]	Maternal-effect lethal	Near −8			Uncloned
lsy-16	*ot158*	Class I	43	16	None obvious	Near 4			Uncloned
lsy-9	*ot85*	Class V	20	38	None obvious		Temperature sensitive		Uncloned
	ot136		50				Temperature sensitive		Uncloned
	ot202		50				Temperature sensitive		Uncloned
	ot210		20		None obvious				Uncloned

(*continued*)

TABLE 3

(Continued)

Locus	Allele	Class	ASEL marker defect (%)	ASER marker defect (%)	Obvious pleiotropies	Map position	Notes	Nucleotide change	Sequence
						Linkage group V			
lsy-6	ot71	Class II	100	100	None obvious	2.63		JOHNSTON and HOBERT (2003)	
	ot182		100		None obvious			Deletion (precise boundaries not determined)	
	ot149		100		Sick			G > T	gatttttatgagacc
	ot150		20		None obvious			C > T	ttacggctttcgccca
lsy-12	ot89	Class II	86	95	Low brood size, Egl	2.20–2.26		Uncloned	
	ot154		42		None obvious			Uncloned	
	ot170		100		Unc, Pvl			Uncloned	
	ot185		90		Egl			Uncloned	
	ot171		100		Bags, sick, mild Pvl		Fails to complement ot89, but complements other lsy-12 alleles	Uncloned	
lsy-19	ot177[b]	Class II	50	42	None obvious	Near 0		Uncloned	
lsy-20	ot219	Class IV	0[j]	35	None obvious	4–5		Uncloned	
						Linkage group X			
ceh-36	ot79	Class II	48	49	None obvious	16.66	Temperature sensitive	CHANG et al. (2003)	
lsy-23	ot233	Class VI	80[g]		None obvious	Left of −17		Uncloned	
lsy-2	ot64[d]	class II	100	100	Ste	−17.08		JOHNSTON and HOBERT (2005)	
	ot65[d]		95	97	Ste			JOHNSTON and HOBERT (2005)	
	ot67		96	100	Ste			JOHNSTON and HOBERT (2005)	
	ot72		91	96	Ste			JOHNSTON and HOBERT (2005)	
	ot77		86	100	Ste			JOHNSTON and HOBERT (2005)	
	ot90		86	100	None obvious			G > A	TGC GAA **ATG** AGT TCT

New, uncloned genes are underlined. Class VI mutants are separately shown in Tables 5–7 (except lsy-23 and lsy-24). If not indicated otherwise, scoring of mutant phenotypes for all newly described mutants was done at 25°. In most cases the sample size for each genotype is >50. "ASEL marker defect" indicates percentage of animals with loss of lim-6^{prom}::gfp or gcy-7^{prom}::gfp expression in ASEL (for class II and class III mutants), gain of gfp expression in ASER (for class I and class IV mutants), loss of ASER expression in class V mutants, and ectopic expression in non-ASEL/R cells in class VI mutants. "ASER marker defect" indicates the percentage of animals with loss of gcy-5^{prom}::gfp in ASER (class I and class III mutants) or gain of gfp expression in ASEL (for class II and class IV mutants). Wild-type animals show 0% defects in expression of these markers (n > 100). In the Sequence column, spaces indicate codons; bold indicates mutation; capital letters indicate coding sequences; non-capital letter indicate intronic or promoter sequence. The effect of the nucleotide change in terms of amino acid change is shown in Figure 3. If the mutant allele has been previously described, a reference is given instead.

[a] Scored at 20° owing to lethality.

[b] ot192 worms were scored for ASER fate using the extrachromosomal gcy-5^{prom}::mcherry array otEx2333 crossed with otIs114 animals. Only those animals that produced progeny containing the array were scored.

[c] ot114 worms displaying a 2 ASEL phenotype were scored for ASER fate using the extrachromosomal gcy-5::cherry array otEx2333, crossed with otIs114 animals. One hundred percent of the 2 ASEL worms failed to express gcy-5^{prom}::rfp, indicating that the penetrance of the ASER defect is at the very least 75% (equaling penetrance of 2 ASEL phenotype).

[d] The che-1(ot94) and che-1(ot95) allele pair and the lsy-2(ot64) and lsy-2(ot65) allele pairs likely arose from the same mutagenic event as they were each retrieved from the same "F$_1$ plate" (containing one to two F$_1$ from mutagenized parents); they are each counted as just one allele in the overall screen statistics.

[e] Identifiable ot59 homozygous progeny of heterozygous mothers were scored from a strain balanced with hT2[qIs48]. All ot243 progeny of identified but nonbalanced heterozygous mothers were scored and the numbers corrected for the presence of 1/4 homozygous offspring.

[f] Evidence for being cog-1 or die-1, respectively: mapping data, noncomplementation, and, in the case of cog-1, fosmid rescue (see text).

[g] Defect only with lim-6^{prom}::gfp, not with gcy-7^{prom}::gfp.

[h] See Table 7 for more detail on phenotypes.

[i] The ASEL phenotype is a sum of the phenotypes shown in Figure 2B; the ASER phenotype is the loss of gcy-5^{prom}::gfp expression in ASER.

[j] Indicates that ASEL fate is still expressed. In the case of lsy-20, the absolute level ASEL marker lim-6^{prom}::gfp is, however, decreased in 50% of the animals (assayed with otIs114).
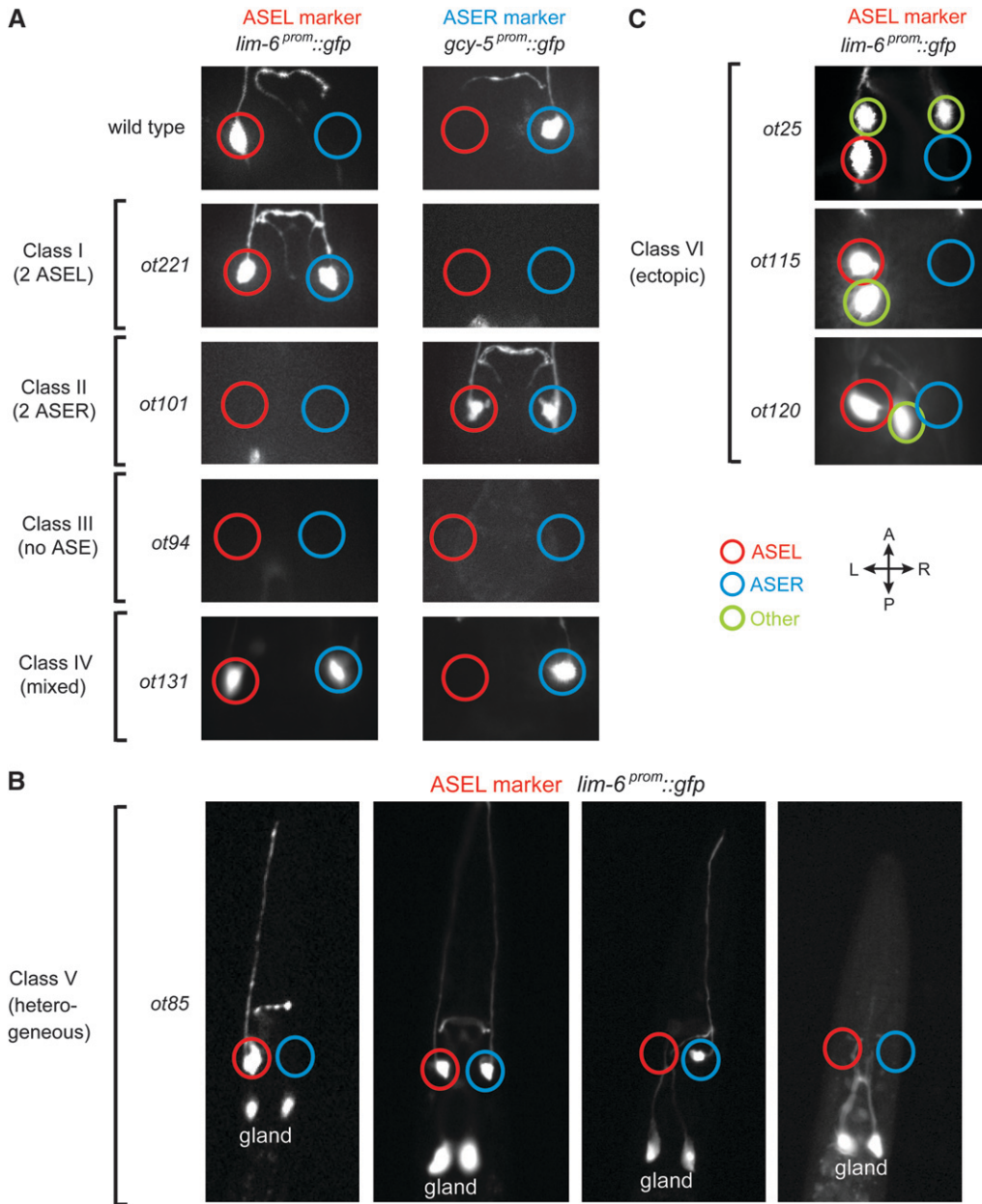
FIGURE 2.—Abnormal expression of left/right asymmetric *gfp* reporter genes in mutant classes ("Lsy phenotype"). Representative examples of mutant phenotypes observed in adult animals are shown. (A) New alleles of the previously described phenotypic classes I–IV. The quantification of defects is shown in Table 3. (B) Heterogeneous phenotypes observed within a population of animals carrying a new, representative class V allele, *ot85*. The two additional cells labeled are the excretory gland cells that normally also express *lim-6* (HOBERT *et al.* 1999). The occurrence of each phenotypic category in *ot85* mutants is: *lim-6*^prom^*::gfp (otIs114)* in ASEL only, 40% (100% in wild-type animals); ASEL and ASER, 28%; ASER only, 12%; neither ASEL nor ASER, 20% ($n = 109$). The ASER marker *gcy-5*^prom^*::gfp* shows only one mutant category, "ASER off," in 38% of animals ($n = 112$). (C) Representative allele of the new mutant class VI. The quantification of defects is shown in Tables 3, 5, and 6.

screened; Table 1), we aimed to identify temperature-sensitive alleles of known genes that would help us address the question of at what stage the previously described regulatory factors (Figure 1B) act to control ASE fate determination. We indeed found that five alleles of *cog-1* show a strong temperature-sensitive phenotype. All five alleles harbor the same Ala > Val substitution that is highly conserved in most homeodomain proteins (Figure 4A) and is located in the third α-helix of known homeodomain structures (Figure 4B) (PIPER *et al.* 1999). A slightly more bulky Val residue in this position may affect the packing of the three α-helixes, thereby possibly destabilizing the protein at higher temperatures. We note that a mutation in an adjacent position of the homeodomain of UNC-4 (Leu > Phe) also causes a

temperature-sensitive phenotype (MILLER *et al.* 1993). Other less specific impacts of Ala > Val mutations, *e.g.*, on protein synthesis, cannot be ruled out.

We characterized one of these alleles, *ot221*, in more detail. *ot221* animals raised at 15° show an almost 100% penetrant wild-type phenotype, while animals raised at 25° show a ~50% penetrant 2 ASEL phenotype (Figure 4C). By performing both up- and downshift experiments at different developmental stages we found that *cog-1* gene activity is required embryonically only right around or shortly after the birth of the ASE neurons to control terminal ASEL and ASER fate, as assessed by the expression of three different differentiation markers (Figure 4D). Raising or lowering *cog-1* gene activity after the threefold stage has no effect on the expression of the

three terminal differentiation markers that we tested (Figure 4D).

These temperature-shift experiments demonstrate that the bistable feedback loop, of which *cog-1* is a critical component, is required only embryonically to initiate the induction of the L/R asymmetric, terminal differentiation features of ASEL and ASER. After this initial choice has been made, terminal differentiation features must rely on some other mechanisms to maintain their activity. This finding is perhaps unexpected since feedback loops are often involved in stabilizing and maintaining cellular fates (EDLUND and JESSELL 1999) and since the expression of bistable loop components, including *cog-1*, persists in ASE throughout adulthood, as measured by various reporter gene constructs (data not shown). Given our temperature-shift experiments, we speculate that the ASE feedback loop may rather act to amplify an initial, perhaps transient or low-level input into the system, rather than stabilizing it. Fate stabilization and maintenance may be ensured by positive autoregulation of transcription factors that provide the output from the loop (*die-1*) or act downstream of the loop, such as *lim-6*, which we have previously shown to autoregulate (JOHNSTON *et al.* 2005). Moreover, we note that in a newly isolated allele of the class IV gene *fozi-1*, a transcription factor, the mutant phenotype appears more penetrant in adult *vs.* larval stage animals (*ot191* allele), which argues for a continuous requirement of the gene throughout larval and adult stages. The lack of requirement for the bistable feedback loop postembryonically may also explain a puzzling observation that we previously reported, namely that in *lim-6* mutants, *lsy-6* expression is partially lost without having an effect on expression of terminal fate markers such as *gcy-7* (JOHNSTON *et al.* 2005). We infer that the loss of *lsy-6* in *lim-6* mutants occurs too late to have an impact on the temporally restricted, ASEL-inducing activity of *lsy-6*.

unc-37: In addition to class I *cog-1* alleles, we isolated two recessive alleles of the *unc-37* Groucho-type transcriptional cofactor (Table 3; Figure 3). Both alleles cause an embryonic lethal phenotype that is maternally rescued. The Lsy phenotype is not maternally rescued and can be readily observed in the homozygous offspring of heterozygous mothers (Table 3).

FIGURE 3.—Molecular identity of mutant alleles. Alleles first described in this article are shown in green and alleles that we previously described (CHANG *et al.* 2003; JOHNSTON and HOBERT 2003, 2005; JOHNSTON *et al.* 2006) are shown in purple. See Figures 4 and 5 for alleles in non-protein-coding regions of genes (*lsy-6* and *cog-1* 3′-UTR). The nucleotide changes for all mutations are shown in Table 3. Two pairs of alleles, *lsy-2(ot64)* and *lsy-2(ot65)* (JOHNSTON and HOBERT 2005) as well as *che-1(ot94)* and *che-1(ot95)* were isolated from the same plate and have very likely arisen from the same mutagenic event. Allele counts in Table 2 and Figure 7 include only one allele per allele pair. Note that current Wormbase (WS160) and GenBank entries show an incorrect gene structure of *che-1* that does match the experimentally determined cDNA structure, published by UCHIDA *et al.* (2003). Upon reanalyzing the *che-1(ot73)* sequence we found the molecular lesion to be a D233G change, rather than an earlier frameshift, as previously reported (CHANG *et al.* 2003).
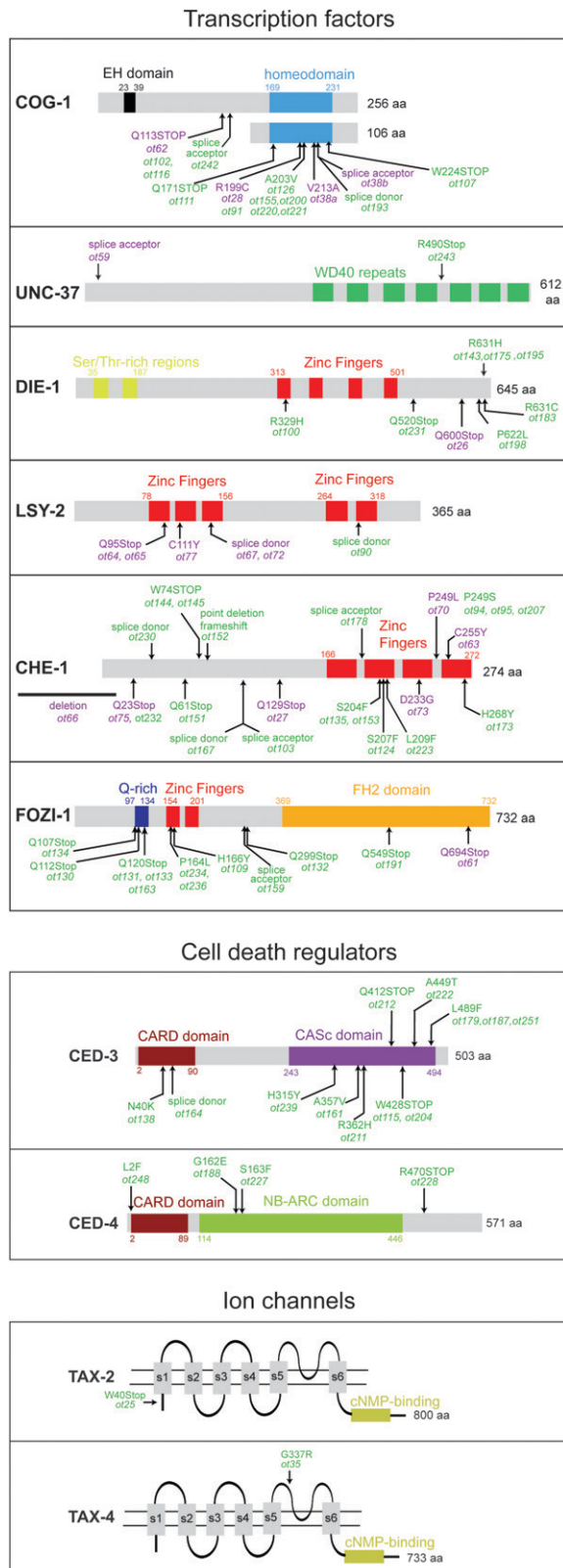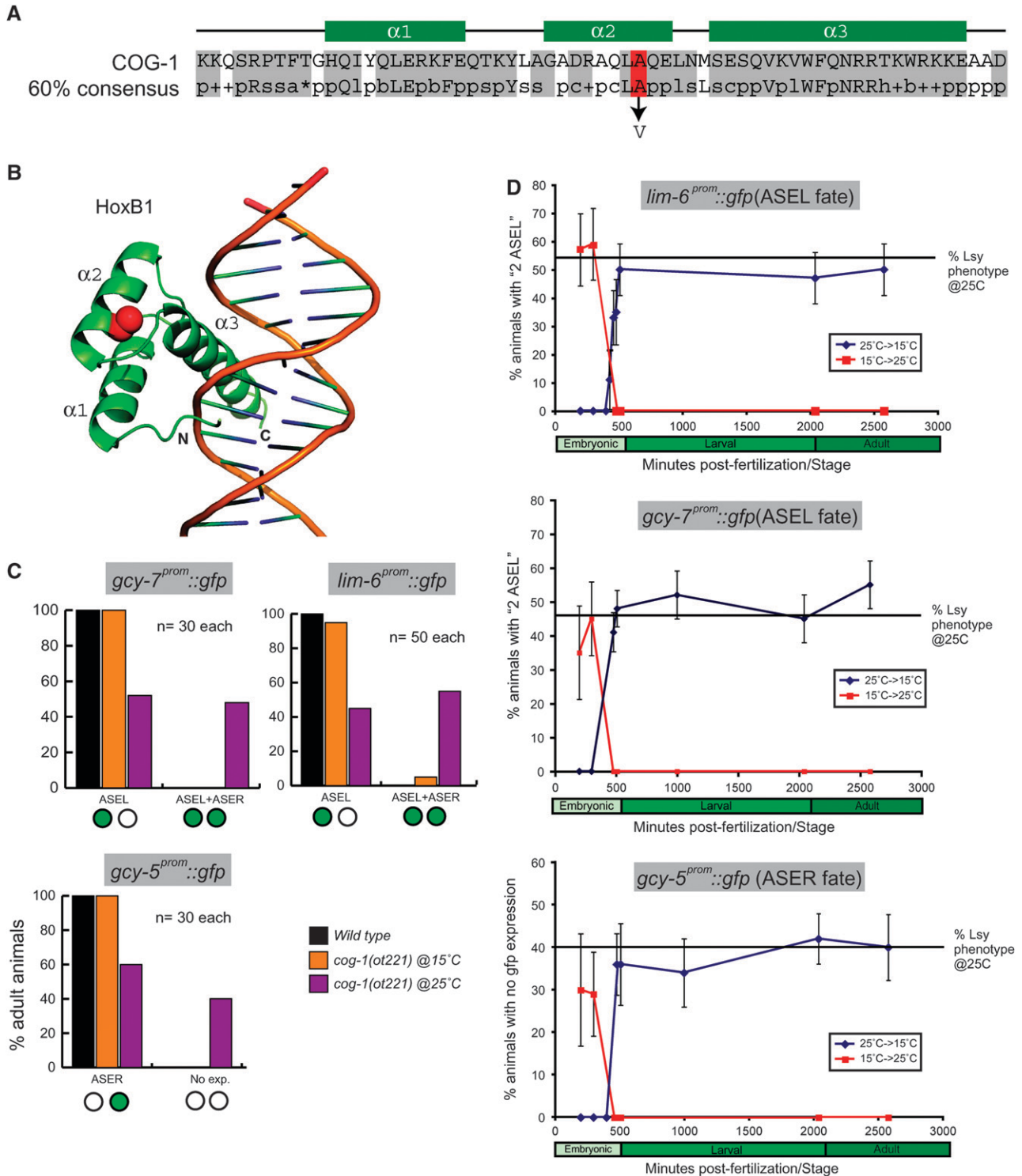
FIGURE 4.—Analysis of the temperature-sensitive *cog-1* allele *ot221*. (A) Alignment of the COG-1 homeodomain to the consensus sequence found in >60% of homeodomains in the SMART database (http://smart.embl-heidelberg.de/). See SMART for abbreviations used. The Ala residue mutated to Val in the five *cog-1* temperature-sensitive alleles (*ot126*, *ot155*, *ot200*, *ot220*, and *ot221*) is shown. Secondary structure elements are indicated according to PIPER *et al.* (1999). (B) Structure of HoxB1 bound to DNA (PIPER *et al.* 1999). The structure was obtained from http://www.pdb.org/pdb/explore/explore.do?structureId=1B72. The alanine residue that is mutated in COG-1 is indicated in a ball model. (C) *cog-1(ot221)* animals show a temperature-sensitive Lsy phenotype as assessed with *otIs3* (*gcy-7prom::gfp*), *otIs114* (*lim-6prom::gfp*), and *ntIs1* (*gcy-5prom::gfp*). Animals were kept at the indicated temperatures for several generations. (D) Temperature-shift experiments with terminal differentiation markers *otIs3* (*gcy-7prom::gfp*), *ntIs1* (*gcy-5prom::gfp*), and *otIs114* (*lim-6prom::gfp*). All animals were scored as adults. Animals that were temperature shifted postembryonically had been staged by Clorox-mediated extraction of eggs from gravid adults. Embryonically shifted animals were also staged by Clorox-mediated extraction of embryos from gravid adults, but picked specifically at the two-cell stage. The phenotype of non-temperature-shifted animals (from C) is shown as a black line.

On the basis of their physical interactions in other systems as well as genetic interaction tests, we proposed that the COG-1 and UNC-37 proteins directly interact to control the postmitotic adoption of terminal ASEL and ASER fates (CHANG *et al.* 2003). However, a recent analysis of maternal *unc-37* function in the early embryo reveals a role for this gene in early, Notch-mediated lineage decisions (NEVES and PRIESS 2005). *unc-37* acts as a corepressor with the *ref-1* family of bHLH transcription factors downstream of Notch signaling in the early embryo. In *ref-1* mutants, a second ectopic ASEL neuron is generated from the ABara blastomere (POOLE and HOBERT 2006). To test whether the cell that ectopically expresses ASEL fate in hypomorphic *unc-37(e262)* mutants (CHANG *et al.* 2003) is caused by an early lineage transformation in the ABara lineage or whether it is caused by the transformation of the ABp-derived ASER neuron into ASEL, we laser ablated the ABp blastomere in *unc-37(e262)* mutants. This manipulation abolished one of the two cells that expresses ASEL fate, which indicates that this cell is not derived from the ABara blastomere and which is consistent with this cell being ASER (data not shown). Taken together, *unc-37* functions independently of its early embryonic patterning role to cause a 2 ASEL phenotype.

New class I mutants: In addition to *cog-1* and *unc-37* alleles, we found six recessive class I mutations that define four novel class I complementation groups, termed *lsy-5, lsy-16, lsy-17,* and *lsy-22* (Table 3, supplemental Table 2 at http://www.genetics.org/supplemental/). Up to two alleles per locus were identified. The penetrance of the mutant phenotypes ranges from 35 to 100% penetrant (Table 3). *lsy-16* and *lsy-17* are fertile and viable, while the *lsy-5* and *lsy-22* genes are required for viability. The embryonic lethality of *lsy-22* mutants is maternally rescued but the Lsy phenotype is not. The most severe allele of *lsy-5* mutants, *ot37*, displays zygotic embryonic and larval lethality. Escapers are uncoordinated (Unc) and display a protruding vulva (Pvl) phenotype but produce no progeny. A weaker allele of *lsy-5, ot240,* is homozygous viable but also Unc and Pvl.

We previously noted that mutations in the first two identified class I genes, *cog-1* and *unc-37,* failed to complement each other (CHANG *et al.* 2003). The nonallelic noncomplementation is likely a reflection of a direct physical interaction of COG-1 and UNC-37 proteins, which we infer from the ability of COG-1 orthologs (Nkx6 family) to physically interact via the EH1 domain with vertebrate UNC-37 orthologs (MUHR *et al.* 2001). Nonallelic noncomplementation is, however, not a general feature shared by class I genes. For example, *lsy-5* and *lsy-16* each complement *unc-37* and the new class I *lsy* genes show complementation among each other (supplemental Table 2 at http://www.genetics.org/supplemental/).

Future molecular characterization and genetic epistasis analysis will reveal how *lsy-5, lsy-16, lsy-17,* and *lsy-22* fit into the known regulatory architecture of ASE fate specification shown in Figure 1B. Given that they fall into the same phenotypic category as *cog-1*, it is possible that some of these genes may mediate the control of the *die-1* 3′-UTR by the *cog-1* gene. Our previous work indicated that *cog-1* may exert its effect on the *die-1* 3′-UTR through *mir-273,* a miRNA that is expressed in a *cog-1*-dependent manner in ASER and that is sufficient to downregulate *die-1* expression (CHANG *et al.* 2004; JOHNSTON *et al.* 2005). However, *mir-273* alleles were not recovered from our screens, perhaps because of a potential redundancy of *mir-273* with several sequence-related miRNAs (*mir-51* through *mir-56*) or because another factor (miRNA or protein) may have a more prominent role in controlling the *die-1* 3′-UTR. In that latter case, it is conceivable that the molecular identity of *lsy-5, lsy-16, lsy-17,* and *lsy-22* will provide a better understanding of how *cog-1* controls the *die-1* 3′-UTR.

Class II mutants (2 ASER neurons)

Alleles of known class II genes: We have isolated a total of 22 recessive alleles of known class II genes (*die-1, lsy-2, ceh-36, lin-49,* and *lsy-6*) and one gain-of-function allele of a previously described class I gene, *cog-1*.

die-1: *die-1* encodes a C2H2 Zn-finger transcription factor (HEID *et al.* 2001). In contrast to the early embryonic lethality of a *die-1* null mutant allele (HEID *et al.* 2001), all *die-1* alleles that we isolated are viable and all except one of the *die-1* alleles show a 100% penetrant Lsy phenotype (Table 3). With the exception of *ot100*, a point mutation in the first Zn finger, all other alleles cluster at the C terminus of the protein and constitute either nonsense or missense mutations (Figure 3). This C-terminal region contains no recognizable sequence motif, but missense mutations alter residues that are conserved in three nematode species (data not shown). Considering the viability of these alleles and their completely penetrant Lsy phenotype, it is possible that these alleles have revealed genetically separable functions of distinct parts of the DIE-1 protein. For example, the C terminus of DIE-1 may interact with a cell-type-specific cofactor in ASEL. Alternatively, all of these alleles may simply produce less overall gene activity and the essential function of *die-1* in the hypodermis (HEID *et al.* 2001) may require less gene activity than *die-1* function in the ASE neurons.

lsy-2: *lsy-2* encodes a C2H2 Zn-finger transcription factor (JOHNSTON and HOBERT 2005). All previously described alleles of *lsy-2* cause a completely penetrant sterility (Ste) phenotype, whose basis is currently unknown (JOHNSTON and HOBERT 2005). We have now also recovered an allele, *ot90*, a splice donor mutation (Figure 3), which displays the Lsy but not the Ste phenotype.

cog-1: We mapped the only dominant gain-of-function mutation retrieved in our screen, *ot123* [48% penetrant 2 ASER phenotype in heterozygous state ($n = 114$);

FIGURE 5.—A gain-of-function mutation in the *cog-1* locus. (A) Location of the *ot123* mutation. The *ot123* deletion does not eliminate the *lsy-6* complementary site but deletes a second, less strongly conserved *lsy-6* complementary site that we previously noted (JOHNSTON and HOBERT 2003) (light red shading). Further analysis of the 3′-UTR revealed that a region apart from this second site, also contained within the *ot123* deletion, appears to be required for downregulation of the 3′-UTR (D. DIDIANO and O. HOBERT, unpublished data). (B) 3′-UTR sensor data. Each tripartite bar graph classifies *gfp* expression from the 3′-UTR sensor into three categories: L > R, more *gfp* expression in ASEL than in ASER; L = R, *gfp* expression in ASEL and ASER is equal; L < R, less *gfp* expression in ASEL than in ASER. As controls, we rescored the *unc-54* 3′-UTR control transgenic line *otEx2646*, described in DIDIANO and HOBERT (2006) (not regulated, *i.e.*, no bias in expression in ASEL *vs.* ASER), and we scored a new *cog-1* 3′-UTR control transgenic line (*otIs185*, a chromosomally integrated version of one of the previously described extrachromosomal lines in DIDIANO and HOBERT 2006; expression is strongly biased to ASER). Only single control lines were scored since previous work showed no variance between lines (DIDIANO and HOBERT 2006). Several independent lines (*otEx3076–otEx3078*) were tested for the *cog-1* 3′-UTR*ot123* sensor and each showed nonregulated expression compared to the *unc-54* 3′-UTR or any other nonregulated 3′-UTR (DIDIANO and HOBERT 2006).

100% penetrant in homozygous state ($n = 76$)] to the *cog-1* locus. Sequence analysis revealed a 329-bp deletion that eliminates the last 105 bp of the *cog-1* 3′-UTR (Figure 5A). The *cog-1* 3′-UTR is downregulated in ASEL by the *lsy-6* miRNA (JOHNSTON and HOBERT 2003) and ectopic expression of *cog-1* in ASEL transforms ASEL into ASER (CHANG *et al.* 2003). A failure to downregulate endogenous *cog-1* expression therefore causes the same 2 ASER phenotype that we observe in *ot123* animals (Table 3). To experimentally test whether the 3′-UTR deletion in *ot123* mutants indeed causes a failure to downregulate the *cog-1* 3′-UTR, we employed a previously described sensor gene strategy (JOHNSTON and HOBERT 2003; DIDIANO and HOBERT 2006). In this approach the ASEL/ASER-expressed promoter of the *ceh-36* gene is fused to *gfp*, followed by the *cog-1* 3′-UTR. This sensor construct is downregulated in ASEL and this downregulation can be observed by assessing relative *gfp* levels in ASEL *vs.* those in ASER (Figure 5B). Introduction of a deletion into this sensor that corresponds to the *ot123* mutation causes a failure to downregulate *gfp*

expression, and therefore the *cog-1* 3′-UTR, in ASEL (Figure 5B). We conclude that in *cog-1(ot123)* animals, ectopic expression of *cog-1* in ASEL causes the cell to adopt an ASER fate.

We note that the *ot123* deletion does not delete the *lsy-6* complementary site in the *cog-1* 3′-UTR (Figure 5A), which is required for *cog-1* downregulation (JOHNSTON and HOBERT 2003). As the *lsy-6* complementary site is not sufficient to confer downregulation of a 3′-UTR (DIDIANO and HOBERT 2006), we conclude that the *ot123* mutation affects another *cis*-regulatory or structural element of the *cog-1* 3′-UTR that is required for *lsy-6*-mediated downregulation of *cog-1*.

lsy-6: We had previously described the isolation of a single allele of the miRNA *lsy-6*, a deletion allele that eliminates the complete miRNA (*ot71*; Figure 6A) (JOHNSTON and HOBERT 2003). Our expanded screening efforts resulted in the isolation of three more *lsy-6* alleles, two point mutations (*ot149* and *ot150*) and a deletion allele (*ot182*) that eliminates the entire *lsy-6* locus (Figure 6A). All alleles are completely viable, have
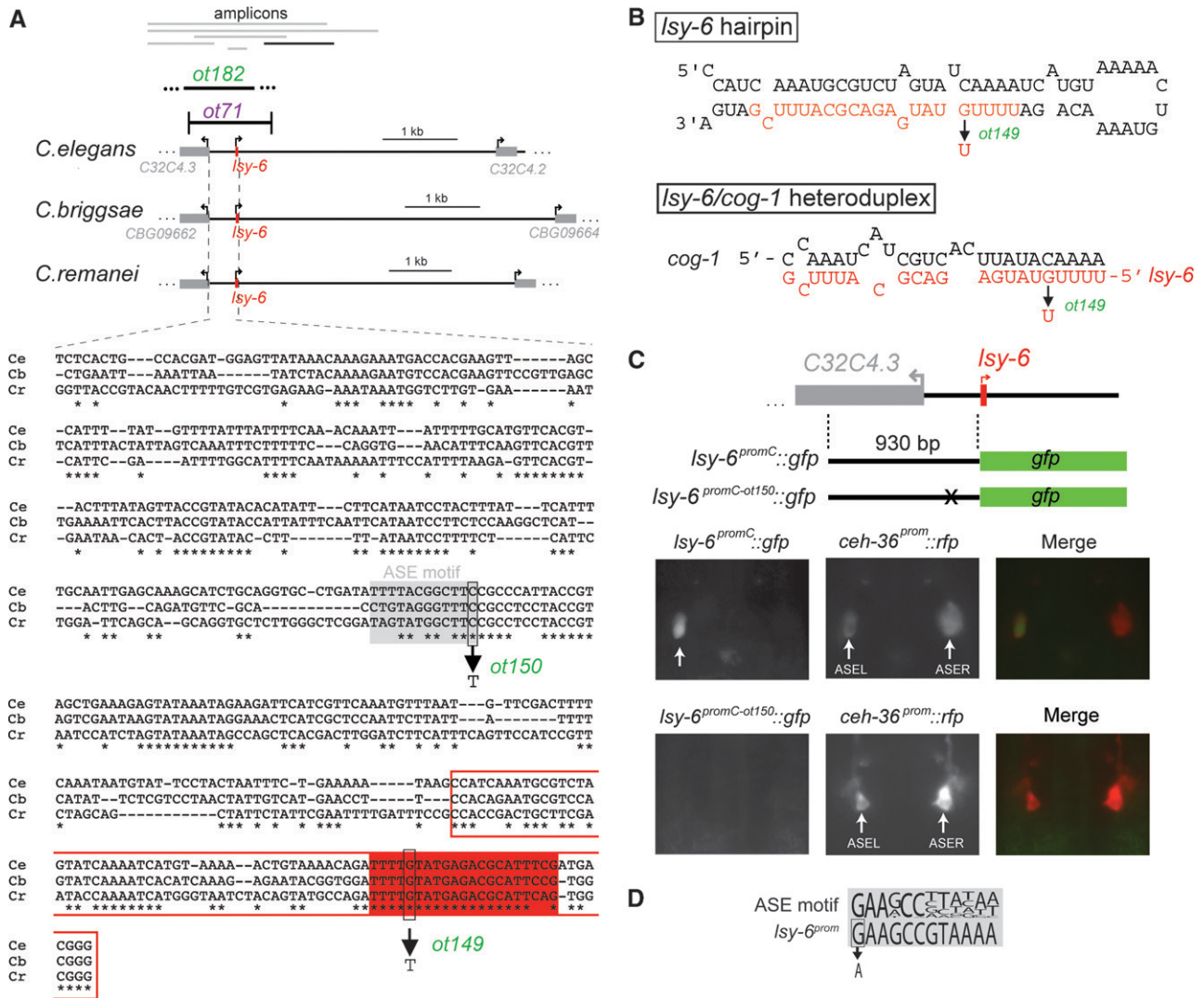
FIGURE 6.—Mutant alleles of the miRNA *lsy-6*. (A) Location of all *lsy-6* alleles. The syntenic region around the *lsy-6* locus in three nematode species is shown. The *lsy-6* hairpin is boxed in red, and the mature miRNA is shaded red (OHLER *et al.* 2004). The *ot71* allele (purple) was described previously, and the *ot149*, *ot150*, and *ot182* alleles (green) are new. The sequence of the *lsy-6* locus and the intergenic region from *lsy-6* to the first predicted exon of the upstream gene is shown and point mutations are indicated. We have not mapped the precise endpoint of *ot182* as we have been unable to obtain PCR products across the *lsy-6* locus. The genomic regions that we attempted to amplify by PCR are indicated at the top; all regions could be amplified from wild-type genomic DNA, the amplicon indicated in black could also be amplified from *ot182* genomic DNA lysates, while the amplicons indicated in gray could not be amplified from *ot182* lysates. Corroborating the notion that *ot182* is a *lsy-6* allele, *ot182* fails to complement *lsy-6(ot71)* and maps to the *lsy-6* locus. See D for more information on the gray-shaded ASE motif. (B) The *ot149* mutation disrupts the seed region in the *cog-1/lsy-6* heteroduplex and also affects base pairing in the *lsy-6* hairpin precursor. (C) Functional analysis of the *lsy-6(ot150)* allele. The *ot150* mutation disrupts expression of a *lsy-6* reporter gene fusion. Four of five *lsy-6^promC^::gfp* lines show expression in ASEL (12–33% penetrant; see MATERIALS AND METHODS for comments on this transgene) and zero of four *lsy-6^promC-ot150^::gfp* show expression in ASEL. (D) The *ot150* mutation affects one of the invariant positions in the ASE motif, a binding site for the Zn-finger transcription factor CHE-1 (ETCHBERGER *et al.* 2007). The ASE motif of *lsy-6* binds CHE-1 *in vitro* (ETCHBERGER *et al.* 2007). CHE-1 is required to induce the hybrid precursor state in the two ASE neurons during which asymmetric regulatory and terminal differentiation factors are initially expressed in a bilateral manner (JOHNSTON *et al.* 2005). The ASE motif shown here is consensus build from >20 ASE expressed genes (ETCHBERGER *et al.* 2007).

normal brood sizes, and display no obvious pleiotropies. With a total of four alleles, the allele frequency of the *lsy-6* locus is one in 24,000 haploid genomes. The only two other cloned genes besides *lsy-6* whose null phenotype does not impinge on brood size, overall health, or viability are more frequently isolated (*che-1*, 1/5400; *fozi-1*,

1/10,000; Table 2) but as these protein-coding loci are also much larger than *lsy-6* they are more likely to be targeted by a random mutagen.

The *ot149* point mutation in the *lsy-6* locus is a G > U substitution. The mutated G nucleotide normally participates in base pairing within the *lsy-6* hairpin precursor

TABLE 4

***ceh-36* mutants show a temperature-sensitive Lsy phenotype**

		"2 ASER" phenotype[b]			
		15°		25°	
Genotype	Nature of allele[a]	% animals	*n*	% animals	*n*
Wild type		0	>100	0	>100
ceh-36(ot79)		88	50	12	51
ceh-36(ky640)		78	50	44	75
ceh-36(ky646)		52	54	0	56
ceh-36(tm251)		Embryonic lethal			
ceh-36(ok795)		Embryonic lethal			

[a] Boxes indicate exons of the *ceh-36* locus (5′ to left), red filling indicates position of the homeobox. Solid arrows indicate premature stop codons (CHANG *et al.* 2003; LANJUIN *et al.* 2003), open arrows indicate deletion alleles (http://www.wormbase.org).

[b] Scored with the *ntIs1* transgene. Worms were grown at 15° or 25° for several generations and scored as adults. The original scoring of *ot79* mutants, grown at 20° and reported by Chang *et al.* is shown in Table 3. Ectopic expression of the *ntIs1* marker in ASEL of *ceh-36* mutants is often much dimmer than normal expression in ASER.

(Figure 6B, top) and in base pairing between the mature *lsy-6* miRNA with its complementary sequence in the *cog-1* 3′-UTR (Figure 6B, bottom).

In contrast to the other *lsy-6* alleles, the *lsy-6(ot150)* allele is only weakly penetrant (Table 3) and, like the *ot149* and *ot182* alleles, was identified as a *lsy-6* allele by noncomplementation with the *lsy-6* reference allele *ot71* (data not shown). *lsy-6(ot150)* animals harbor a C → T mutation ∼100 nucleotides upstream of the predicted *lsy-6* hairpin structure (Figure 6A). We considered the possibility that the mutation might affect a *cis*-regulatory element required for *lsy-6* expression. Consistent with such a possibility, the alignment of the *lsy-6* upstream region in *C. elegans*, *C. briggsae*, and *C. remanei* reveals that the *ot150* allele lies in a conserved patch of nucleotides, consistent with this region being functionally relevant (Figure 6A). To test the functional relevance of this region experimentally, we introduced this mutation into a reporter gene construct that monitors expression of *lsy-6* in the ASEL neuron. The introduction of this mutation completely abolishes expression of the reporter in ASEL (Figure 6C). The *ot150* mutation therefore indeed disrupts a *cis*-regulatory element required for *lsy-6* expression.

A recent analysis of *cis*-regulatory elements of genes expressed in ASE identified a *cis*-regulatory element, termed the ASE motif, that is required for expression of genes in ASE and constitutes a binding site for the Zn-finger transcription factor CHE-1 (ETCHBERGER *et al.*

2007). The *ot150* mutation affects one of the invariant positions of the ASE motif (Figure 6D).

ceh-36 and lin-49: Notably, we did not recover additional alleles of the previously described *lin-49* and *ceh-36* genes, two transcription factors required for expression of the ASEL fate (CHANG *et al.* 2003), even though we have screened ∼10 times as many haploid genomes as in the previously described smaller-scale screens. Since our original publication of the only *ceh-36* allele that resulted from our initial screen, *ot79* [a premature stop codon very late in the coding sequence (CHANG *et al.* 2003)], two additional, also completely viable alleles of *ceh-36*, *ky640*, and *ky646*, have become available (LANJUIN *et al.* 2003). Both *ky640* animals and *ot79* mutant animals harbor a premature stop codon late in the gene, and each allele displays a partially penetrant class II (2 ASER) phenotype (CHANG *et al.* 2003; LANJUIN *et al.* 2003). In contrast, the *ky646* allele, which harbors a premature stop codon at the beginning of the homeobox, was reported to display a much weaker Lsy phenotype (LANJUIN *et al.* 2003). To exclude that this surprising result is not caused by different scoring criteria or conditions in different laboratories, we compared adult mutant animals side-by-side at carefully controlled temperatures. We observed that all alleles display a previously unnoted strong temperature sensitivity with a much stronger phenotype at 15°, compared to 25° (Table 4). This is particularly evident for *ky646* animals, which display no phenotype at 25°, but a >50% penetrant

phenotype at 15°. This observation suggests that *ky646*, in spite of its premature stop codon, may not be a null allele. Indeed, two *ceh-36* deletion alleles, independently isolated by two different knockout consortia, display embryonic lethality (http://www.wormbase.org), which likely represents the true null phenotype of the gene. Such a phenotype is consistent with an early embryonic expression of *ceh-36* at epidermal closure (data not shown). Moreover, RNAi of *ceh-37*, a closely related paralog of *ceh-36* (LANJUIN *et al.* 2003), shows no effect on viability or ASE laterality in a wild-type background, but causes embryonic lethality if done in a viable *ceh-36(ky646)* mutant background (data not shown). Taken together, the cold sensitivity and early embryonic pleiotropy of *ceh-36* gene function may decrease the frequency of allele recovery in our screens, which were mainly conducted at 25°. Pleiotropies that affect the viability of strong *lin-49* loss-of-function alleles (CHAMBERLIN and THOMAS 2000; CHANG *et al.* 2003) may also explain the low recovery rate of *lin-49* mutants.

New class II mutants: We recovered nine class II mutant alleles that define four novel class II genes, *lsy-12*, *lsy-14*, *lsy-15*, and *lsy-19* (Table 3, supplemental Table 2 at http://www.genetics.org/supplemental/). All five loci are recessive, viable, and defined by one to five alleles, ranging in penetrance from 50 to 100% (Table 3). One viable mutant, *lsy-12(ot86)*, has the unique property of being maternally rescued as revealed by scoring the homozygous progeny of heterozygous parents. An egg-laying-defective (Egl) phenotype associated with *lsy-12* is not maternally rescued.

Future molecular characterization and genetic epistasis analysis will reveal how *lsy-12, lsy-14, lsy-15,* and *lsy-19* fit into the known regulatory architecture of ASE fate specification (Figure 1B). As these genes show similar phenotypes to the *lsy-6* miRNA, it is conceivable that one of these loci may be a miRNA-specific cofactor of *lsy-6* activity that may provide a better understanding of miRNA function. Such cofactors are beginning to emerge from other systems (NOLDE *et al.* 2007). As expected, we have not retrieved generic miRNA processing enzymes, such as Dicer, due to early development pleiotropies associated with loss of these genes (GRISHOK *et al.* 2001). As is the case for novel class I genes, the novel class II genes described here may also act far outside the bistable feedback loop to provide a link between the early embryonic Notch induction and the bistable feedback loop (? in Figure 1B). An early embryonic function is a particularly attractive possibility for *lsy-12*, which appears to be contributed maternally.

Class III mutants (no ASEL/R differentiation)

All class III mutants that we identified define a single complementation group on chromosome I, *che-1* (Figure 3; Table 3), which codes for a Zn-finger transcription factor (CHANG *et al.* 2003; UCHIDA *et al.* 2003). We have

identified a total of 22 *che-1* alleles, which include splice site, missense, and nonsense mutations in the coding region of the gene (Figure 3). All of the nonsense mutations are located before the C-terminal Zn-finger domains. All of the amino acid-changing missense mutations reside in three of the four Zn-finger domains (Zn-finger 2, 3, and 4). We have recently shown that Zn-finger 3 and 4, but not Zn-finger 1 and 2, are involved in binding of CHE-1 to the ASE motif of the *gcy-5* gene (ETCHBERGER *et al.* 2007). The ASE motif is a *cis*-regulatory element that is present in many ASE-expressed promoters (ETCHBERGER *et al.* 2007). The apparent requirement of Zn-finger 2 for ASE development, revealed by our genetic analysis, suggests that CHE-1 may show a differential domain requirement for binding to different ASE motifs.
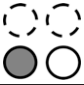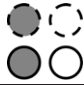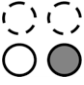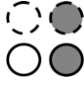
The loss of genes that control the tightly regulated expression of *che-1* in ASE (CHANG *et al.* 2003; UCHIDA *et al.* 2003) would be expected to yield a class III mutant phenotype, yet no class III mutants other than *che-1* were found. We presume that either those upstream regulators have pleiotropies that prevented their retrieval (*e.g.*, essential functions in early embryonic development) or a redundant set of regulatory factors may control *che-1* expression.

Class IV mutants (mixed fate of ASEL or ASER neurons)

Alleles of known class IV genes: We have previously identified two genes with a class IV "mixed" phenotype, the LIM homeobox gene *lim-6* and the C2H2 Zn-finger factor *fozi-1* (HOBERT *et al.* 1999; JOHNSTON *et al.* 2006). In *lim-6* mutants, ASER fate is ectopically expressed in ASEL without the concomitant complete loss of ASEL fate, while in *fozi-1* mutants, ASEL fate markers are ectopically expressed in ASER without the concomitant loss of ASER fate markers (schematically shown in Figure 1A). Our extended screening efforts have retrieved 11 additional alleles of *fozi-1*, many of them premature stop codons (Table 3; Figure 3). Two missense mutations map into the first Zn-finger domain, thereby corroborating its previously reported importance in *fozi-1* function (JOHNSTON *et al.* 2006). No missense mutations in the FH2 domain were identified, corroborating our previous conclusion that the FH2 domain is not essential for *fozi-1* function (JOHNSTON *et al.* 2006). The *ot191* and the *ot61* allele, both nonsense mutations in the FH2 domain, may destabilize the mRNA and/or protein. Animals that carry the *ot191* allele show a more penetrant phenotype in adult compared to larval stages (data not shown), suggesting that *fozi-1* may be continuously required to maintain ASER fate.

We have not isolated any alleles of the LIM homeobox gene *lim-6*, a previously known class IV gene. This gene was the first regulatory gene to be implicated in ASE laterality, on the basis of the analysis of a single, reverse-genetically engineered deletion allele, *nr2073*, which

TABLE 5

ASE cell fate in cell death mutants

Gene	Allele	% animals expressing ASEL fate marker (*otIs114*)			*n*	Nucleotide change	Sequence context[b]
Wild type		100	0	0	>100		
ced-3	*n717*[a]	5	95	0	40		
	ot115	10	90	0	52	G > A	GTT TCG T**G**A AGA AAC
	ot138	20	80	0	56	T > G	AGT GAT AA**G** GGA GAT
	ot161	5	95	0	58	C > T	GTG CAG G**T**T TGT CGA
	ot164	8	92	0	54	G > A	CCAGATC**a**taggtttttaa
	ot179	10	90	0	67	C > T	CGC CTG **T**TC AAA AAG
	ot187	31	69	0	55	C > T	CGC CTG **T**TC AAA AAG
	ot204	11	89	0	62	G > A	GTT TCG T**G**A AGA AAC
	ot211	22	78	0	63	G > A	GGC GAA C**A**T CGT GAC
	ot212	16	84	0	51	C > T	CCG AGC **T**AA GCT GAC
	ot222	32	68	0	53	G > A	ACA CAC **A**CA AAG GAT
	ot239	58	42	0	62	C > T	CTA TCA **T**AC GGA GAA
	ot251	15	85	0	52	C > T	CGC CTG **T**TC AAA AAG
ced-4	*n1162*[a]	5	96	0	45		
	ot188	34	66	0	53	G > A	CGA GCT G**A**A TCC GGA
	ot227	33	67	0	54	C > T	GCT GGA **T**TC GGA AAA
	ot228	12	88	0	57	C > T	GGA AAA **T**GA ATG CCC
	ot238	44	57	0	71	No mutation in coding region[c]	
	ot248	13	87	0	60	C > T	tcag ATG **T**TC TGC GAA

Gene	Allele	% animals expressing ASER fate marker (*ntIs1*)			*n*		
Wild type		100	0	0	>100		
ced-3	*n717*[a]	5	95	0	50		
ced-4	*n1162*[a]	4.5	95.5	0	50		

All animals were scored at 25°. Circles indicate ASEL and ASER, and dashed circles indicate ASEL/R sisters that are fated to die. Gray shading indicates *gfp* expression.

[a] Reference allele.

[b] Spaces indicate codons, boldface type indicates mutation, uppercase letters indicate coding sequences, and lowercase letters indicate intronic sequence. See Figure 3 for amino acid change.

[c] Evidence for being *ced-4* is noncomplementation with reference allele and linkage to the *ced-4* locus.

eliminates the complete DNA-binding domain of *lim-6* (HOBERT *et al.* 1999). *lim-6(nr2073)* mutants show only partially penetrant and expressive effects on the expression of the *gfp* markers that we used for screening (JOHNSTON *et al.* 2005, 2006), thereby providing a possible explanation for our failure to retrieve *lim-6* alleles.

New class IV mutants: We have identified three novel class IV mutant loci, *lsy-18*, *lsy-20*, and *lsy-26* (Table 3). The mutant phenotypes of both *lsy-20* and *lsy-26* are defined by the ectopic expression of the ASER marker *gcy-5* in ASEL. In contrast to class II mutants, the ectopic expression of the ASER marker is not accompanied by a loss of expression of the ASEL fate marker (Table 3). The ASEL neuron therefore displays a mixed fate, characterized by coexpression of ASEL and ASER fate markers. This phenotype is similar to that of *lim-6(nr2073)* mutants (HOBERT *et al.* 1999). *lim-6* has distinct func-

tions in different neuron types (HOBERT *et al.* 1999). It is conceivable that *lsy-20* and *lsy-26* are transcription factors that may act together with *lim-6* to determine its ASE-specific function in controlling *gcy* and *flp* gene expression patterns in ASEL (Figure 1B). Neither *lsy-20* nor *lsy-26* share the Egl phenotype of *lim-6* that is caused by loss of *lim-6* function in the uterus (HOBERT *et al.* 1999).

In contrast to *lsy-20* and *lsy-26*, *lsy-18* displays a *fozi-1*-like mixed phenotype in which ASEL fate is derepressed in ASER without a concomitant loss of the ASER fate marker *gcy-5*. Like in *fozi-1* mutants (JOHNSTON *et al.* 2006), the derepression of ASEL fate in ASER is fully penetrant (100% of animals show derepression of *lim-6^prom^::gfp* in ASER) but only partially expressive (levels of ectopic *gfp* expression in ASER vary and often do not reach the level of expression normally seen in ASEL). *lsy-18* may act together with *fozi-1* to distinguish between

TABLE 6

Regulation of ASE fate markers by the ion channels *tax-2* and *tax-4*

Genotype		Ectopic ASEL marker *lim-6* ^{prom}*::gfp*		Ectopic ASEL marker *gcy-7* ^{prom}*::gfp*		Ectopic ASER marker *gcy-5* ^{prom}*::gfp*	
		% animals	n	% animals	n	% animals	n
Wild type		0	>100	0	>100	0	>100
tax-4	*p678*[a]	86	22	0	56	0	40
	ot35	100	35	ND		ND	
tax-2	*p691*[b]	48	48	0	90	0	23
	ot25	72	53	ND		ND	

All worms were grown at 20° and scored as adults. ND, not determined.

[a] Early stop and putative null (Komatsu *et al.* 1996).

[b] Missense mutation with most severe behavioral phenotype (Coburn and Bargmann 1996).

the roles of *fozi-1* in neuronal and mesodermal cell specification (Johnston *et al.* 2006; Amin *et al.* 2007).

Class V mutants (heterogeneous phenotype)

We recovered five alleles with novel phenotypes. Four of these alleles define a new complementation group on chromosome IV, termed *lsy-9*, which displays a heterogeneous phenotype. Within a population of mutant animals, a spectrum of phenotypes is observed, including the loss of the ASEL marker *lim-6*, ectopic expression of *lim-6* in ASER, and, surprisingly, exclusive expression of *lim-6* in ASER (Figure 2B; Table 3). The ASER fate marker *gcy-5* is frequently lost, but never ectopically expressed in ASEL (Table 3).

One allele, *ot147*, defines a new locus on chromosome II, *lsy-21*, which displays another type of a heterogeneous phenotype that varies within a population. Some animals lose expression of the ASEL marker *lim-6* in ASEL while a subset of these animals also lose expression of the bilateral ASEL/R marker *ceh-36* in ASEL but not in ASER (data not shown), indicating a partial loss of ASE cell fate.

At this point it is difficult to speculate on the potential role of class V genes. It is conceivable that these mixed phenotypes reflect a reduced but not completely eliminated gene dosage. The characterization of null phenotypes of these loci will eventually resolve this issue.

Class VI mutants (ectopic ASEL/R fate)

We identified a substantial number of mutants that display normal L/R asymmetric expression of the ASE fate markers in the ASE neurons, but ectopic expression of ASEL or ASER markers in cells other than ASEL or ASER (Figure 2C). In spite of the normal ASEL/R laterality, we still refer to this phenotype as a Lsy phenotype as the mutants were isolated with *gfp* markers that monitor ASEL/R laterality.

Cell death mutants: The sisters of ASEL and ASER normally undergo programmed cell death (Sulston

et al. 1983). We retrieved a substantial number of alleles of previously known regulators of cell death, namely 12 alleles of *ced-3* and 5 alleles of *ced-4* (Yuan *et al.* 1993; Shaham and Horvitz 1996; Figure 3). All alleles display ectopic expression of ASEL fate markers in the undead sister of ASEL (Figure 2; Table 5). Similarly, undead ASER sisters execute the ASER fate (Table 5). Although we found that a reference loss-of-function allele of the cell death gene *egl-1* also causes a class VI phenotype (data not shown), we did not retrieve *egl-1* alleles, possibly because the locus is very small (Conradt and Horvitz 1998). Undead cells have previously been shown to execute the fate of their lineal sisters (*e.g.*, Avery and Horvitz 1987; Guenther and Garriga 1996). In the case of the ASE neurons, the observation that the undead ASEL or ASER sister cell expresses the appropriate fate [rather than being "stuck" in the bilateral ASE precursor state (Johnston *et al.* 2005)] provides a further argument for left/right asymmetric fate being programmed into the ASEL and ASER lineage before the ASE neurons are generated (Poole and Hobert 2006). Also, it argues that the cleavage plane of the last cell division generating the ASE neurons has no impact on the adoption of ASE fate (*i.e.*, both the anterior and the posterior daughter of the ASE mother cell can adopt the ASE fate).

Ion channel mutants: Two mutant alleles displayed normal expression of *lim-6* in ASEL, but also ectopic expression in a pair of bilaterally symmetric sensory neurons located anteriorly to ASE, the AFD thermosensory neurons (Figure 2C; Table 6). Mapping and complementation tests revealed that these mutations affect the two subunits of a previously identified, AFD-expressed cyclic nucleotide gated ion channel, *tax-2* and *tax-4* (Figure 3, Table 6) (Coburn and Bargmann 1996; Komatsu *et al.* 1996). Unlike previously described *tax-2* alleles, *tax-2(ot25)* appears to be a clear molecular null allele (early stop codon; Figure 3). Similar defects in the expression of the ASEL fate marker *lim-6* can be observed using previously described reference alleles of *tax-2* and *tax-4* (Table 6). Ectopic expression of ASE fate in AFD is

TABLE 7

The ABp blastomere generates ectopic ASER neurons in *lsy-25* mutants

Genotype	Cell fate marker[a]	Laser ablation	% animals with number of *gfp*-positive cells equaling[b]				
			0	1	2	3	*n*
Wild type[c]	ASER marker	Mock ablated	2	98	0	0	64
		ABp ablated	95	5	0	0	22
	ASEL marker	Mock ablated	0	55	45	0	22
		ABp ablated	21	75	4	0	24
lsy-25(ot97)	ASER marker	Mock ablated	37	44	19	0	43
		ABp ablated	100	0	0	0	9
	ASEL marker	Mock ablated	47	6	47	0	17
		ABp ablated	100	0	0	0	7

[a] ASER marker, *ntIs1* (*gcy-5^{prom}::gfp*); ASEL marker, *otIs3* (*gcy-7^{prom}::gfp*).

[b] At this point it is unclear whether the zero *gfp*-expressing cell category indicates that ASE is formed, but does not express the respective marker or whether the embryo has died prior to the generation of ASE. In all cases, the embryos were allowed to develop for 12–15 hr.

[c] These data are taken from POOLE and HOBERT (2006) and shown for comparison only.

restricted to the *lim-6* gene. Neither the ASEL marker *gcy-7*, nor the ASER marker *gcy-5*, nor the bilateral ASEL/R marker *ceh-36* display any expression defects in *tax-2/tax-4* mutants (Table 6 and data not shown).

Loss of *tax-2/tax-4* was previously shown to affect gene expression of a putative olfactory receptor in the ASI and AWC neurons (TROEMEL *et al.* 1999; PECKOL *et al.* 2001); an effect of these channels on the regulation of gene expression is therefore not unprecedented. However, in contrast to the previously described case, the expression of *lim-6* in AFD is not controlled by the calcium-dependent UNC-43 kinase since neither gain- nor loss-of-function mutations in the *unc-43* gene affect *lim-6* expression (CHANG *et al.* 2003).

New mutants: We identified mutations in two genes on LGII and LGX, termed *lsy-23* and *lsy-24*, that show normal ASEL/R laterally but display ectopic *lim-6^{prom}::gfp* expression in the AVL motor neuron (Figure 2C). As is the case for *tax-2/tax-4*, the ectopic expression is observed only with the *lim-6* fate marker and not with the alternative ASEL marker *gcy-7^{prom}::gfp* (data not shown).

We isolated a single allele of a gene on LGIV, termed *lsy-25(ot97)*, which displays a completely penetrant embryonic lethal phenotype that is maternally rescued. Homozygous *lsy-25* embryos derived from a heterozygous mother show no aberrant ASEL/R specification, but the unviable offspring of these animals show up to two *gcy-5^{prom}::gfp*-expressing cells (wild-type animals at similar embryonic stages of development always show only one *gcy-5^{prom}::gfp*-expressing cell) and up to two *gcy-7^{prom}::gfp*-expressing cells [two is normal for wild-type animals as mature ASEL markers label both ASE neurons in the embryo (POOLE and HOBERT 2006)] (Table 7). The apparent 2 ASER phenotype of this mutant is, however, not caused by a transformation of ASEL into ASER (as in class II mutants), but caused by a lineage transformation within the ABp lineage. In wild-type animals, the ASER neuron is generated from ABp and the ASEL neuron

from ABa. ABa ablation in wild-type animals therefore eliminates ASEL and ABp ablation eliminates ASER (Table 7) (POOLE and HOBERT 2006). In *lsy-25(ot97)* animals, the ablation of ABp eliminates both *gcy-5^{prom}::gfp*-expressing cells (Table 7). As ASEL is derived from ABa, the ectopic *gcy-5^{prom}::gfp* cell can therefore not be an ASEL > ASER transformed neuron, but is rather a descendant of the ABp lineage that normally produces ASER.

lsy-25(ot97) animals not only generate an additional ASER cell from the ABp lineage, but also lack the normally ABa-derived ASEL neuron. We derived this notion from laser ablation of ABp in *lsy-25(ot97)* animals expressing *gcy-7^{prom}::gfp*, which normally marks both ASEL and ASER in embryos. ABp ablation completely eliminates *gcy-7^{prom}::gfp* expression. We conclude that in *lsy-25(ot97)*, the ABa lineage fails to produce an ASEL neuron, while a lineage transformation in ABp generates an ectopic ASE lineage that expresses the ASER fate. We therefore classify *lsy-25* as a class VI mutant.

Saturation of the screens

Having determined the number of complementation groups recovered by our screens, we considered the degree of saturation of our genetic screens. Hints about saturation are contrasting: On the one hand, (a) 13 nucleotide positions in six different loci have been hit multiple times (one even five times; summarized in supplemental Table 3 at http://www.genetics.org/supplemental/), (b) multiple alleles of the small miRNA *lsy-6* have been retrieved, (c) several loci are represented by >10 alleles (Figure 7), and (d) viable hypomorphic alleles of essential genes (*e.g.*, *die-1*, *lin-49*, *lsy-5*) have been isolated. On the other hand, eight loci are represented only by single alleles (Figure 7). These eight single-allele loci do not reside within a particular class (Table 2, Figure 7), indicating that alleles of any one class are not harder to
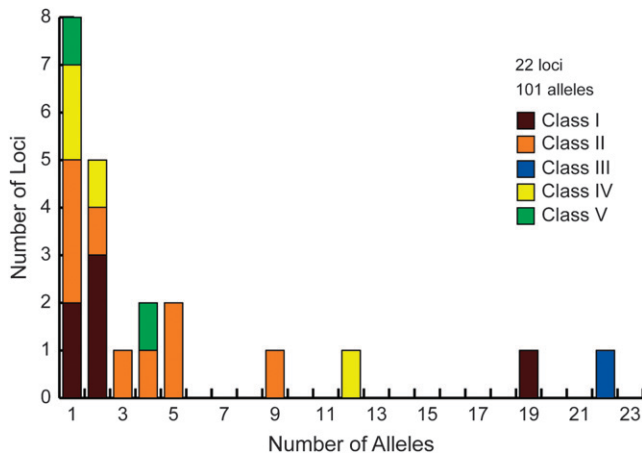
Figure 7.—Saturation of the genetic screen. Distribution of number of complementation groups against the number of mutants isolated per locus is shown. We did not include class VI genes in the analysis as these do not disrupt the developmental program in ASEL or ASER.

uncover than others. Genes defined by single alleles may have pleiotropic functions and these single alleles may be rare alleles that do not provide enough activity for their function in ASE development but do provide enough activity for other functions.

To analyze the degree of saturation in a more quantitative manner, we utilized a method introduced by POLLOCK and LARKIN (2004) that calculates the maximum-likelihood estimates of the number of alleles that remain to be found. The algorithm attempts to fit the given data (number of alleles *vs.* number of loci) to various models that describe a different probability of discovering mutants across the genome. The model that fits our allele distribution the best predicts a 74% saturation of our screen (supplemental Table 3 at http://www.genetics.org/supplemental/), indicating that up to 12 class I–class V loci in addition to the currently known 23 class I–class V loci (Table 2) remain to be identified. We caution that this is only a rough estimate that does not take into account 34 mutants with a <10% penetrant mutant phenotype. Future analysis of these mutants may increase allele coverage for several loci, thereby causing a different saturation estimate.

Conclusions

One approach to understanding how cellular diversity in the nervous system is genetically encoded is to employ genetically amenable model systems to screen for mutants in which developmental programs in the nervous system are disrupted. This endeavor has been substantially aided by the introduction of reporter gene technology that allows the visualization of the differentiation program of neurons on a single-cell level in live animals (CHALFIE *et al.* 1994). We have made use of *gfp* reporter gene technology to dissect the genetic pro-

gram of a single-neuron class-specific fate decision at unprecedented genetic depth. In light of an average allele frequency of 1/2000 haploid genomes (ANDERSON 1995), our screening through ∼120,000 mutagenized haploid genomes provides a broad catalog of genes that govern ASE cell fate specification. Our screens also recovered informative alleles of previously known genes, such as a conditional *cog-1* allele that allowed us to demonstrate that a previously described bistable feedback loop is required to initiate but not to maintain terminal fates. This is an unexpected finding in light of the persistent expression of bistable loop components throughout the life of the animal. The retrieval of hypomorphic alleles of essential genes further illustrates the advantage of genetic screens over genomewide knockout approaches that would not have revealed functions of several genes due to early pleiotropies. Apart from the previously known 10 loci that control ASE specification, we have identified 16 novel loci and estimate that another 12 loci remain to be identified. We expect that the molecular characterization of all these loci will continue to provide insights into the architecture of gene regulatory networks that induce and maintain neuronal cell fate decisions.

LITERATURE CITED

AMIN, N. M., K. HU, D. PRUYNE, D. TERZIC, A. BRETSCHER *et al.*, 2007 A Zn-finger/FH2-domain containing protein, FOZI-1, acts redundantly with CeMyoD to specify striated body wall muscle fates in the Caenorhabditis elegans postembryonic mesoderm. Development **134:** 19–29.

ANDERSON, P., 1995 Mutagenesis, pp. 31–58 in *Caenorhabditis elegans: Modern Biological Analysis of an Organism*, edited by H. F. EPSTEIN and D. SHAKES. Academic Press, New York/London/San Diego.

AVERY, L., and H. R. HORVITZ, 1987 A cell that dies during wild-type C. elegans development can function as a neuron in a ced-3 mutant. Cell **51:** 1071–1078.

BARGMANN, C. I., and H. R. HORVITZ, 1991 Chemosensory neurons with overlapping functions direct chemotaxis to multiple chemicals in C. elegans. Neuron **7:** 729–742.

BRENNER, S., 1974 The genetics of *Caenorhabditis elegans*. Genetics **77:** 71–94.

CHALFIE, M., Y. TU, G. EUSKIRCHEN, W. W. WARD and D. C. PRASHER, 1994 Green fluorescent protein as a marker for gene expression. Science **263:** 802–805.

CHAMBERLIN, H. M., and J. H. THOMAS, 2000 The bromodomain protein LIN-49 and trithorax-related protein LIN-59 affect development and gene expression in Caenorhabditis elegans. Development **127:** 713–723.

CHANG, S., R. J. JOHNSTON, JR. and O. HOBERT, 2003 A transcriptional regulatory cascade that controls left/right asymmetry in chemosensory neurons of C. elegans. Genes Dev. **17:** 2123–2137.

Chang, S., R. J. Johnston, C. Frokjaer-Jensen, S. Lockery and O. Hobert, 2004 MicroRNAs act sequentially and asymmetrically to control chemosensory laterality in the nematode. Nature **430:** 785–789.

Coburn, C. M., and C. I. Bargmann, 1996 A putative cyclic nucleotide-gated channel is required for sensory development and function in C. elegans. Neuron **17:** 695–706.

Conradt, B., and H. R. Horvitz, 1998 The C. elegans protein EGL-1 is required for programmed cell death and interacts with the Bcl-2-like protein CED-9. Cell **93:** 519–529.

Davis, M. W., M. Hammarlund, T. Harrach, P. Hullett, S. Olsen *et al.*, 2005 Rapid single nucleotide polymorphism mapping in C. elegans. BMC Genomics **6:** 118.

Didiano, D., and O. Hobert, 2006 Perfect seed pairing is not a generally reliable predictor for miRNA-target interactions. Nat. Struct. Mol. Biol. **13:** 849–851.

Edlund, T., and T. M. Jessell, 1999 Progression from extrinsic to intrinsic signaling in cell fate specification: a view from the nervous system. Cell **96:** 211–224.

Etchberger, J. F., A. Lorch, M. C. Sleumer, R. Zapf, S. J. Jones, *et al.*, 2007 The molecular signature and cis-regulatory architecture of a *C. elegans* gustatory neuron. Genes Dev. **21:** 1653–1674.

Good, K., R. Ciosk, J. Nance, A. Neves, R. J. Hill *et al.*, 2004 The T-box transcription factors TBX-37 and TBX-38 link GLP-1/Notch signaling to mesoderm induction in C. elegans embryos. Development **131:** 1967–1978.

Grishok, A., A. E. Pasquinelli, D. Conte, N. Li, S. Parrish *et al.*, 2001 Genes and mechanisms related to RNA interference regulate expression of the small temporal RNAs that control C. elegans developmental timing. Cell **106:** 23–34.

Guenther, C., and G. Garriga, 1996 Asymmetric distribution of the C. elegans HAM-1 protein in neuroblasts enables daughter cells to adopt distinct fates. Development **122:** 3509–3518.

Heid, P. J., W. B. Raich, R. Smith, W. A. Mohler, K. Simokat *et al.*, 2001 The zinc finger protein DIE-1 is required for late events during epithelial cell rearrangement in C. elegans. Dev. Biol. **236:** 165–180.

Hobert, O., 2006 Architecture of a microRNA-controlled gene regulatory network that diversifies neuronal cell fates. Cold Spring Harbor Symp. Quant. Biol. **71:** 181–188.

Hobert, O., K. Tessmar and G. Ruvkun, 1999 The Caenorhabditis elegans lim-6 LIM homeobox gene regulates neurite outgrowth and function of particular GABAergic neurons. Development **126:** 1547–1562.

Hobert, O., R. J. Johnston, Jr. and S. Chang, 2002 Left-right asymmetry in the nervous system: the Caenorhabditis elegans model. Nat. Rev. Neurosci. **3:** 629–640.

Hodgkin, J., and T. Doniach, 1997 Natural variation and copulatory plug formation in *Caenorhabditis elegans*. Genetics **146:** 149–164.

Johnston, R. J., and O. Hobert, 2003 A microRNA controlling left/right neuronal asymmetry in Caenorhabditis elegans. Nature **426:** 845–849.

Johnston, Jr., R. J., and O. Hobert, 2005 A novel C. elegans zinc finger transcription factor, lsy-2, required for the cell type-specific expression of the lsy-6 microRNA. Development **132:** 5451–5460.

Johnston, Jr., R. J., S. Chang, J. F. Etchberger, C. O. Ortiz and O. Hobert, 2005 MicroRNAs acting in a double-negative feedback loop to control a neuronal cell fate decision. Proc. Natl. Acad. Sci. USA **102:** 12449–12454.

Johnston, Jr., R. J., J. W. Copeland, M. Fasnacht, J. F. Etchberger, J. Liu *et al.*, 2006 An unusual Zn-finger/FH2 domain protein controls a left/right asymmetric neuronal fate decision in C. elegans. Development **133:** 3317–3328.

Komatsu, H., I. Mori, J. S. Rhee, N. Akaike and Y. Ohshima, 1996 Mutations in a cyclic nucleotide-gated channel lead to abnormal thermosensation and chemosensation in C. elegans. Neuron **17:** 707–718.

Lanjuin, A., M. K. VanHoven, C. I. Bargmann, J. K. Thompson and P. Sengupta, 2003 Otx/otd homeobox genes specify distinct sensory neuron identities in C. elegans. Dev. Cell **5:** 621–633.

Miller, D. M., C. J. Niemeyer and P. Chitkara, 1993 Dominant unc-37 mutations suppress the movement defect of a homeodomain mutation in unc-4, a neural specificity gene in Caenorhabditis elegans. Genetics **135:** 741–753.

Muhr, J., E. Andersson, M. Persson, T. M. Jessell and J. Ericson, 2001 Groucho-mediated transcriptional repression establishes progenitor cell pattern and neuronal fate in the ventral neural tube. Cell **104:** 861–873.

Neves, A., and J. R. Priess, 2005 The REF-1 family of bHLH transcription factors patterns C. elegans embryos through Notch-dependent and Notch-independent pathways. Dev. Cell **8:** 867–879.

Nilsen, T. W., 2007 Mechanisms of microRNA-mediated gene regulation in animal cells. Trends Genet. **23:** 243–249.

Nolde, M. J., N. Saka, K. L. Reinert and F. J. Slack, 2007 The Caenorhabditis elegans pumilio homolog, puf-9, is required for the 3′UTR-mediated repression of the let-7 microRNA target gene, hbl-1. Dev. Biol. **305:** 551–563.

Ohler, U., S. Yekta, L. P. Lim, D. P. Bartel and C. B. Burge, 2004 Patterns of flanking sequence conservation and a characteristic upstream motif for microRNA gene identification. RNA **10:** 1309–1322.

Ortiz, C. O., J. F. Etchberger, S. L. Posy, C. Frokjaer-Jensen, S. Lockery *et al.*, 2006 Searching for neuronal left/right asymmetry: genomewide analysis of nematode receptor-type guanylyl cyclases. Genetics **173:** 131–149.

Palmer, R. E., T. Inoue, D. R. Sherwood, L. I. Jiang and P. W. Sternberg, 2002 Caenorhabditis elegans cog-1 locus encodes GTX/Nkx6.1 homeodomain proteins and regulates multiple aspects of reproductive system development. Dev. Biol. **252:** 202–213.

Peckol, E. L., E. R. Troemel and C. I. Bargmann, 2001 Sensory experience and sensory activity regulate chemosensory receptor gene expression in Caenorhabditis elegans. Proc. Natl. Acad. Sci. USA **98:** 11032–11038.

Pflugrad, A., J. Y. Meir, T. M. Barnes and D. M. Miller, 3rd, 1997 The Groucho-like transcription factor UNC-37 functions with the neural specificity gene unc-4 to govern motor neuron identity in C. elegans. Development **124:** 1699–1709.

Pierce-Shimomura, J. T., S. Faumont, M. R. Gaston, B. J. Pearson and S. R. Lockery, 2001 The homeobox gene lim-6 is required for distinct chemosensory representations in C. elegans. Nature **410:** 694–698.

Piper, D. E., A. H. Batchelor, C. P. Chang, M. L. Cleary and C. Wolberger, 1999 Structure of a HoxB1-Pbx1 heterodimer bound to DNA: role of the hexapeptide and a fourth homeodomain helix in complex formation. Cell **96:** 587–597.

Pollock, D. D., and J. C. Larkin, 2004 Estimating the degree of saturation in mutant screens. Genetics **168:** 489–502.

Poole, R. J., and O. Hobert, 2006 Early embryonic programming of neuronal left/right asymmetry in C. elegans. Curr. Biol. **16:** 2279–2292.

Ptashne, M., 1992 *A Genetic Switch*. Blackwell Publishing, Oxford.

Shaham, S., and H. R. Horvitz, 1996 An alternatively spliced C. elegans ced-4 RNA encodes a novel cell death inhibitor. Cell **86:** 201–208.

Sulston, J. E., E. Schierenberg, J. G. White and J. N. Thomson, 1983 The embryonic cell lineage of the nematode Caenorhabditis elegans. Dev. Biol. **100:** 64–119.

Sun, T., and C. A. Walsh, 2006 Molecular approaches to brain asymmetry and handedness. Nat. Rev. Neurosci. **7:** 655–662.

Swan, K. A., D. E. Curtis, K. B. McKusick, A. V. Voinov, F. A. Mapa *et al.*, 2002 High-throughput gene mapping in Caenorhabditis elegans. Genome Res. **12:** 1100–1105.

Troemel, E. R., A. Sagasti and C. I. Bargmann, 1999 Lateral signaling mediated by axon contact and calcium entry regulates asymmetric odorant receptor expression in C. elegans. Cell **99:** 387–398.

Uchida, O., H. Nakano, M. Koga and Y. Ohshima, 2003 The C. elegans che-1 gene encodes a zinc finger transcription factor required for specification of the ASE chemosensory neurons. Development **130:** 1215–1224.

Wicks, S. R., R. T. Yeh, W. R. Gish, R. H. Waterston and R. H. Plasterk, 2001 Rapid gene mapping in Caenorhabditis elegans using a high density polymorphism map. Nat. Genet. **28:** 160–164.

Yu, S., L. Avery, E. Baude and D. L. Garbers, 1997 Guanylyl cyclase expression in specific sensory neurons: a new family of chemosensory receptors. Proc. Natl. Acad. Sci. USA **94:** 3384–3387.

Yuan, J., S. Shaham, S. Ledoux, H. M. Ellis and H. R. Horvitz, 1993 The C. elegans cell death gene ced-3 encodes a protein similar to mammalian interleukin-1 beta-converting enzyme. Cell **75:** 641–652.